15 March 1962 DRL-A-196

THE DETERMINATION OF FARFIELD CHARACTERISTICS OF LARGE, LOW-FREQUENCY TRANSDUCERS FROM NEARFIELD MEASUREMENTS

by

D. D. Baker

Copy No. 74

DRL Acoustical Report No. 196

Resulting from research done under Bureau of Ships
Research and Development Contract NObsr-72627
NE 051247-6, NE 051456-4
Problem 22-C
Sponsored jointly by the Bureau of Ships
and the Office of Naval Research

ABSTRACT

Due to the trend toward large, low-frequency antisubmarine warfare transducers, it has become impossible to make farfield calibration measurements in existing tanks. It has become necessary to find some way of determining farfield characteristics from measurements made near the transducer. It is possible to compute farfield directivity patterns and source levels from pressure amplitude and phase measurements made in the nearfield (at ranges small compared to the transducer dimensions). This can be done with Kirchhoff's formula by using a simple approximation for the normal component of the pressure gradient. Preliminary pattern computations were made on line, plane array, dipole, and line-and-cone transducers from measurements made in an open lake. Extensive pattern and source level computations were made on a large, multi-stave cylindrical (AN/SQS-4 Mod 3) transducer. Measurements were made in open water and in a highly reflective tank while various numbers of the transducer staves were being driven. Agreement with measured values was good throughout and was within ±1 db in the more recent work with the large transducer. Particularly significant is the fact that highly successful measurements were carried out in a tank of diameter only 2.9 times that of the transducer by measuring near the leading edge of the received pulse. This allowed the measurements to be completed before the energy reflected from the tank walls caused interference. Enough detailed practical information is included to enable one to use the techniques. Preliminary work on the development of a simplified nearfield test for a transducer like the AN/SQS-4 Mod 3 is presented. Such a test would enable one to use the nearfield data to make certain judgments about the farfield performance of the transducer without computations.

A C K N O W L E D G M E N T S

The author wishes to express his appreciation to the following persons: Dr. C. W. Horton for his valuable contributions to the theoretical work and his assistance in the editing of this report; Dr. E. Klein, Dr. C. M. McKinney, and Mr. R. H. Wallace for their assistance in the work and in the preparation of this report; Mr. G. S. Innis for his valuable work during the early phases of the project; and Mr. D. B. James and Mr. K. McCormack for their assistance in the work and in the preparation of this report. Special thanks go to Mr. McCormack for his work in the preparation of the Appendix.

Defense Research Laboratory is grateful to the Sonar Branch, Bureau of Ships, and the Acoustics Branch, Office of Naval Research, for the original support on this project. The project presently is supported by the Sonar Branch, Bureau of Ships.

TABLE OF CONTENTS

TABLE OF CONTENTS (CONT'D)

15 March 1962
DDB/lb

I N T R O D U C T I O N

In sonar work the word transducer is used to denote a device that generates acoustic energy in water, or converts acoustic energy in water to electrical energy. In order to use such a device it must be calibrated. A calibration consists of measuring directivity patterns in at least two planes, the source level, the projecting sensitivity, the receiving sensitivity, and the impedance. Normally, all of these quantities except the impedance must be measured with a probe in the farfield or Fraunhofer region. This means the probe must be at a distance greater than the larger of D^2/λ or 10 D where D is the maximum dimension of the aperture of the transducer. The World War II sonar transducers were such that these farfield measurements could be carried out by using pulse techniques in tanks having dimensions of about 20 ft. Since World War II the trend in antisubmarine warfare (ASW) has been toward larger transducers operating at lower frequencies. This has required larger tanks for calibration work. Early in 1959 Defense Research Laboratory began a project to investigate the possibility of determining the directivity pattern and source level of a transducer from measurements made in the nearfield (at ranges small compared to the dimensions of the transducer). The ultimate purpose was the calibration of large, low-frequency transducers in existing tanks, which are too small for farfield measurements.

The theory of computing farfield characteristics from nearfield pressure amplitude and phase measurements was developed and used with success on four types of transducers as a preliminary check. Emphasis was place on computing the characteristics of an AN/SQS-4 Mod 3 transducer because it actually was one of the large ASW transducers. Agreement was very good between measured farfield values and the equivalent farfield values computed from nearfield data obtained in open water. Agreement has been as good as ±1 db when measurements were made in a highly reflective tank having a diameter 2.9 times that of the transducer. The measurements were made by pulsing the transducer and measuring the amplitude and phase near the leading edge of the pulse; that it, before reflected energy from the walls could interfere.

The theory of farfield computations and its application are presented in Chapter I. The remainder of the report contains considerable practical information for those who may desire to use the technique. Chapter II contains general information about measurement instrumentation and the procedure. Chapter III contains specific information about the preliminary work done with the four transducers and the results. Chapter IV presents similar specific information about the AN/SQS-4 Mod 3 transducer, including the tank measurement work. Chapter V makes specific suggestions for the successful use of the technique. Chapter VI describes the preliminary work that has been done on judging farfield performance of a transducer from nearfield data without computations, and Chapter VII summarizes the report.

The Appendix shows the development of numerical formulas and computer flow charts for the computations for each of the transducers used.

15 March 1962
DDB/lb

C H A P T E R I

THE THEORY OF FARFIELD COMPUTATIONS AND ITS APPLICATION

If the pressure in a sound field is of the form

$$p(x,y,z) = a(x,y,z)e^{-i(\omega t-\varphi)} \tag{1}$$

and if the amplitude is not too large, the pressure satisfies the scalar wave equation,

$$\Delta^2 p + k^2 p = 0 \quad . \tag{2}$$

Then the theorem of Kirchhoff[1,2] states that if all of the sources of the sound field are interior to a closed surface S (shown in Dwg. AS-6539), the pressure at any point P exterior to S can be determined by the surface integral

$$p(P) = \frac{1}{4\pi} \iint_S \left[p \frac{\partial}{\partial n}\left(\frac{e^{ikr}}{r}\right) - \left(\frac{e^{ikr}}{r}\right)\frac{\partial p}{\partial n} \right] dS \quad , \tag{3}$$

where $\frac{\partial}{\partial n}$ denotes differentiation with respect to distance along the outward normal to S and r = the distance from P to S,

k = the wave number,

p = the complex pressure on S, and

p(P) = the complex pressure at P

Equation (3) is valid only for sinusoidal fields, as stated in (1), but it is a special case of a general theorem[3] which is valid for sound fields of arbitrary time dependence

---

[1] S. Ballantine, J. Franklin Inst. 221, 469-484 (1936).

[2] B. B. Baker and E. T Copson, The Mathematical Theory of Huygen's Principle (Clarendon Press, Oxford, 1950), 2nd Ed., p. 26

[3] Ibid., p. 35

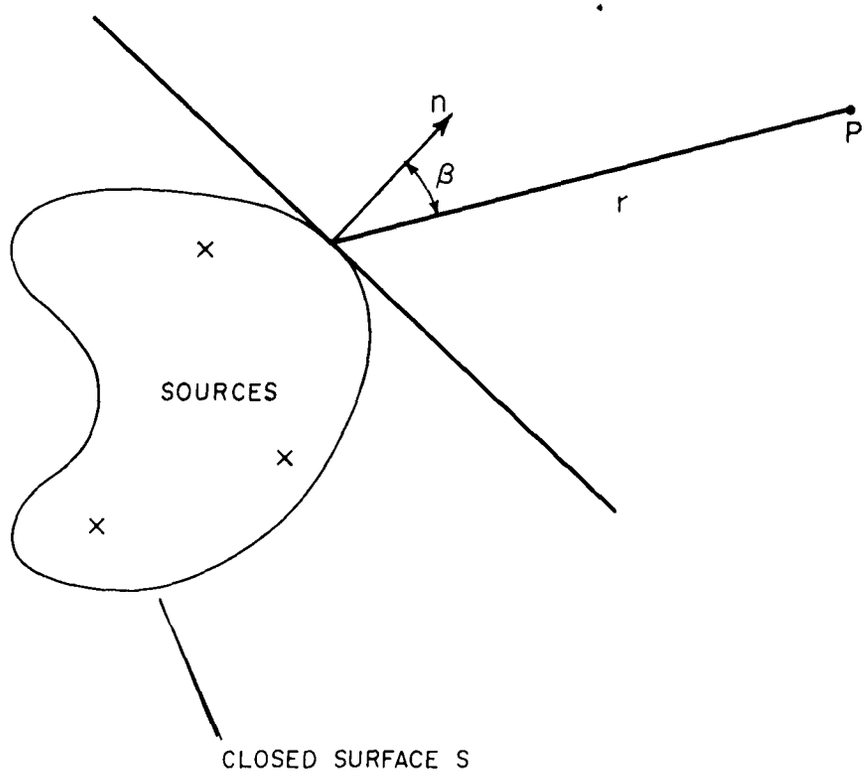

GENERAL SURFACE OF INTEGRATION

DRL – UT
DWG AS 6539
DDB – BBB
3 – 2 – 62

This formula enables one to choose a closed surface near a transducer, to measure the amplitude and phase of p and $\partial p/\partial n$ over the surface, and to determine the pressure at any point in the farfield by evaluating the integral. This evaluation can always be carried out by numerical methods, if necessary. However, the experimental determination of the normal component of the pressure gradient $\partial p/\partial n$ is so difficult that one is tempted to search for a way to avoid the measurement.

To find an expression for $\partial p/\partial n$ which may be substituted into (3), the Newtonian equations of motion may be used. The result of this is the expression of $\partial p/\partial n$ in terms of u_n, the normal component of particle velocity. This quantity is no easier to measure than the normal gradient component.

There is an alternate theoretical approach,[4] based upon finding a suitable Green's function G defined on the surface S and in the space exterior to S, which will enable one to express p(P) in terms of an integral involving P alone. This integral,

$$p(P) = -\frac{1}{4\pi} \iint_S p \frac{\partial G}{\partial n} \, dS \quad , \tag{4}$$

is more simple in appearance than that in (3), but the Green's function conceals some complexity. It is difficult to measure p over surfaces (such as spheres) for which G is easily determined; it is also difficult to find G for surfaces over which p is easy to measure.

The technique that has been used successfully in the work described in this report is to approximate the normal gradient component by ikp. This would be true for plane waves being radiated in the direction of the normal to S.

[4] C. W. Horton and G. S. Innis, "The Computation of Far-Field Radiation Patterns from Measurements Made Near the Source," J. Acoust. Soc. Am., 33, July 1961, pp. 877-880.

Therefore, for a transducer of moderate curvature and a close-fitting surface over which the pressure does not change rapidly, one would suspect the approximation to be valid.

Since the point P is in the farfield and therefore kr is very large compared to unity, it can be shown that

$$\frac{\partial}{\partial n}\left(\frac{e^{ikr}}{r}\right) \cong ik\,\frac{e^{ikr}}{r}\left(\frac{\partial r}{\partial n}\right) \tag{5}$$

where second order terms in $(1/kr)$ have been neglected. The derivative $\partial r/\partial n$ is evaluated at a point on S. The quantity r can be thought of as a scalar field, and $\partial r/\partial n$ can be thought of as the scalar product of the gradient of r and the unit outward normal vector. From these considerations it can be seen that

$$\frac{\partial r}{\partial n} = -\cos\beta \tag{6}$$

where β is the angle between the unit normal and a line connecting P and a point on S. Thus we have the approximation that

$$\frac{\partial}{\partial n}\left(\frac{e^{ikr}}{r}\right) \cong -ik\,\frac{e^{ikr}}{r}\cos\beta \quad . \tag{7}$$

Substituting these approximations into (3) gives

$$p(P) = -\frac{ik}{4\pi}\iint_S (1+\cos\beta)\,\frac{e^{ikr}}{r}\,p\,dS \quad . \tag{8}$$

This expression is that used in the computation of farfield pressures. Although it gives complex pressures in the farfield, magnitudes are determined in order to plot directivity patterns. These magnitudes are computed in absolute pressure units if the nearfield measurements were measured in absolute units.

To this point, measurements and integrations have been considered over closed surfaces. With any closed surface there is no need to measure or to integrate over any portion of the surface where pressures are vanishingly small. This would result in no significant contribution to the integral. Where transducers are plane arrays, the surface of integration may be thought of as a cubical surface with appreciable pressures across only that portion of a plane which passes in front of the active face of the transducer. With cylindrical transducers the ends of the cylindrical surface of integration may be thought of as being included, but pressures are very nearly zero over the ends. Therefore, the surfaces of integration used have been portions of planes, or right circular cylindrical surfaces without ends. Although these are actually only portions of closed surfaces, for practical purposes the theoretical requirement for closed surfaces has not been violated.

To apply this formula to an actual case, an appropriate surface of integration and coordinate system must be selected. For a cylindrical transducer, a cylindrical surface in cylindrical coordinates would be chosen. The length of this surface would depend upon preliminary amplitude measurements. Ideally, the surface should extend to the point where zero pressure is reached. Practically, this would be the point where amplitudes are down 20 to 30 db below the maximum value. The diameter of the surface would depend upon the distance from transducer to probe, which would probably be from 0.25 to about 1.5 wavelengths. If probe distances become too large, the surface must be extended in length to meet the requirement of pressures 20 to 30 db down.

The integral in Equation (8) must be evaluated numerically. Data must be taken over the surface in such numbers as to give an adequate sampling of the pressure. Normally one would suspect that as fewer data were used in the computations, farfield results would gradually become poorer. If data are taken as far apart in space as a wavelength between adjacent points, the computed pattern will contain spurious scallops in it. This is approximately the separation at which individual points start to be resolved. This is the same phenomenon that dictates that the center-to-center spacing of the elements of a transducer array shall be less than about 0.8 wavelength in

order not to resolve the elements.[5] Therefore the separation between adjacent measurement points should in all cases be less than 0.8 wavelength and preferably less than 0.5 wavelength. It would be desirable to make measurements closer together than this depending upon the amount of variation in pressure over the surface. In general, taking more data than necessary for good computed patterns will serve to further improve the accuracy of the patterns and source levels.

There is one exception to the rule of 0.8 wavelength spacing. This rule must always be followed for the spacing between measurement points in the plane of the computed pattern, or in planes parallel to it. However, measurements in lines perpendicular to the plane of the computed pattern need not be spaced this closely. For example, with a cylindrical transducer one might want only patterns in a plane normal to the axis. Data could be taken over the cylinder on three planes which are normal to the axis and two wavelengths apart. In each of these planes, however, data might be taken each three degrees around the transducer in order for the spacing to be 0.5 wavelength. Measurements such as these have been made and used successfully for the computation of patterns. It must be emphasized that with such measurements no pattern in a plane containing the axis can be computed, and that with sampling this sparse along the axis the computed source level values would not necessarily be accurate.

In the Appendix, the development of numerical formulas and computer flow charts from Equation (8) is carried out for each of the transducers for which computations have been made.

---

[5] Design and Construction of Crystal Transducers, Summary Technical Report of Division 6 NDRC, Vol. XXII, p. 137.

15 March 1962
DDB/lb

C H A P T E R I I

GENERAL MEASUREMENT TECHNIQUES

Introduction

This chapter contains general information on the instrumentation and procedures that were used for nearfield and farfield measurements. There is a section listing criteria for choosing suitable hydrophones for nearfield measurements. The systems used for continuous-transmission and pulsed measurements are discussed, as is a proposed addition to the pulsed system. Detailed information on particular sets of measurements will be found in Chapters III and IV.

Nearfield Hydrophones

It is necessary in nearfield measurements to use a hydrophone which is small enough not to create a disturbance in the nearfield. The dimensions of the active face and the overall dimensions perpendicular to the direction of propagation should be 0.25λ or less. Such a probe is moved from point to point in the nearfield in order to make measurements at each point of a desired array. The probe may be stopped at each point while the measurement is made, or it may be moved continuously. In the latter case measurements may be made periodically, or they may be recorded continuously. If continuous recordings are made, data corresponding to the desired points must be read from the recordings.

For a cylindrical transducer, for example, it may be desirable to make measurements around the transducer at three positions along the axis. This may be done by making three passes around the transducer with one probe, or by making one pass around the transducer with three probes connected together. If the probes are also connected in series electrically, the total output is approximately proportional to the integral of the pressure along the length of this makeshift line hydrophone. A true line hydrophone, which effectively is many probes adjacent to each other, gives an output which is a much better approximation of the integral of the pressure along its length. Such a device,

small enough (0.25λ or less) in width and having uniform sensitivity (within ±1 db) along its length, may be used in some cases to make useful nearfield measurements with only one pass around or across the transducer. The hydrophone must be long enough that each end of it extends to where pressures are down as much as 20 to 30 db. If a line hydrophone is used in such a position that its axis is normal to the plane of the pattern to be computed, the integral expression for the farfield pressure contains the integral which the line hydrophone gives directly. Thus the problem is reduced to the numerical evaluation of a line integral. Line hydrophone data can be used only for the computation of patterns in the plane normal to the axis of the line and opposite the center of the active face of the transducer.

Continuous Transmission Measurements

System

The system used for continuous transmission nearfield measurements is shown in Dwg. AS-6491. The transducer was driven with a signal generator and a power amplifier. The output of the probe was amplified to a level suitable for recording on the Brüel and Kjaer recorder. A bandpass filter was used between the amplifier and the recorder to increase the signal-to-noise ratio. Signal level to the recorder was about 1 volt rms with the probe at the position of maximum pressure. This allowed the recorder to track the signal over a dynamic range of some 40 db. An oscilloscope was used to monitor the signal to the recorder.

Since the phasemeter in use required a minimum signal level of 1 volt rms in order to read accurately, it was seen that further amplification of some 40 db would be necessary for accurate phase readings over the same dynamic range. A General Radio Unit Amplifier was used to achieve this high-level amplification. This amplified received signal was applied to one input of the phasemeter; the signal from the signal generator was applied to the other. The phasemeter output was recorded on a dc strip-chart recorder. The dynamic range achieved with this part of the system was adequate for the measurements, although less than the desired 40 db.

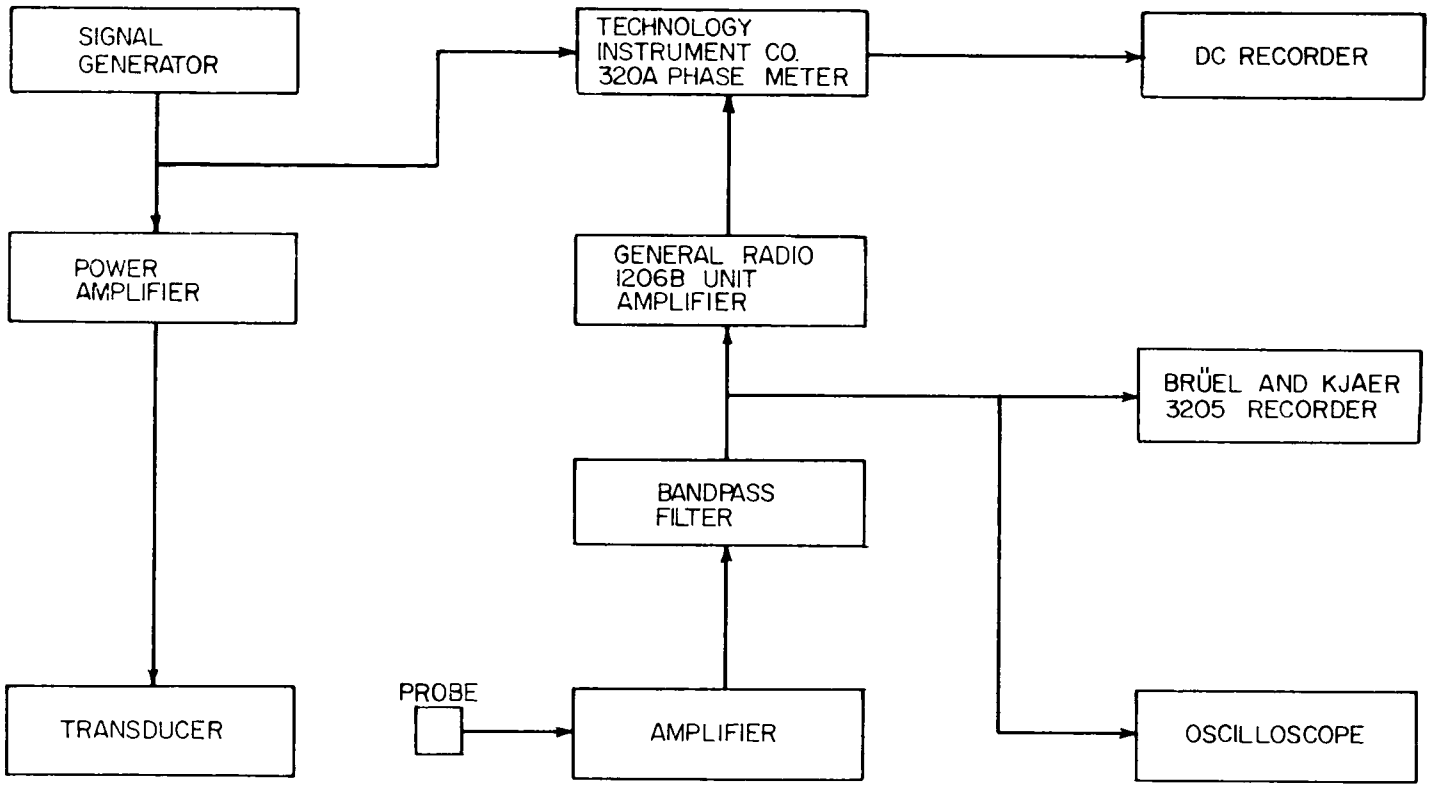

SYSTEM DIAGRAM FOR CONTINUOUS TRANSMISSION
NEARFIELD MEASUREMENTS

DRL - I
DWG AS-64
DDB - Bw
1 - 18 - 6

The system described gave continuous recordings of pressure amplitude and phase as a probe was moved through the nearfield. Because data at discrete points were necessary for the computations, in some cases data were not taken on the recorders. The technique used was to move the probe to a desired position and stop there. Then the amplitude was read from an ac vacuum tube voltmeter in place of the level recorder; the phase was read directly from the phasemeter. In cases where this move-and-stop technique was not feasible, it was necessary to use the recorders and read data from the charts at selected points.

In farfield pattern measurements the amplitude-measuring part of the same system was used; that is, the amplifier, filter, and level recorder were used to make continuous recordings of amplitude.

Procedure

For all continuous-transmission measurements, freefield conditions were necessary on one side of the transducer. The probe or line was placed on the freefield side, and the transducer was rotated in the case of a cylindrical transducer. For a plane transducer, the active face was pointed in the free-field direction and the probe or line moved across the face with a lead-screw device.

In all cases of farfield measurements the transducer was rotated with a suitable hydrophone placed sufficiently far away in the freefield.

Pulsed Transmission Measurements

Original System

As shown in Dwg. AS-6490, a pulse of the signal generator frequency was generated by the transmitter gate of the DRL pulser, and was applied to a power amplifier that drove the transducer. The system generated a pulse each time a switch was closed. The switch was closed mechanically each 3.6 degrees of rotation of the AN/SQS-4 Mod 3 transducer.

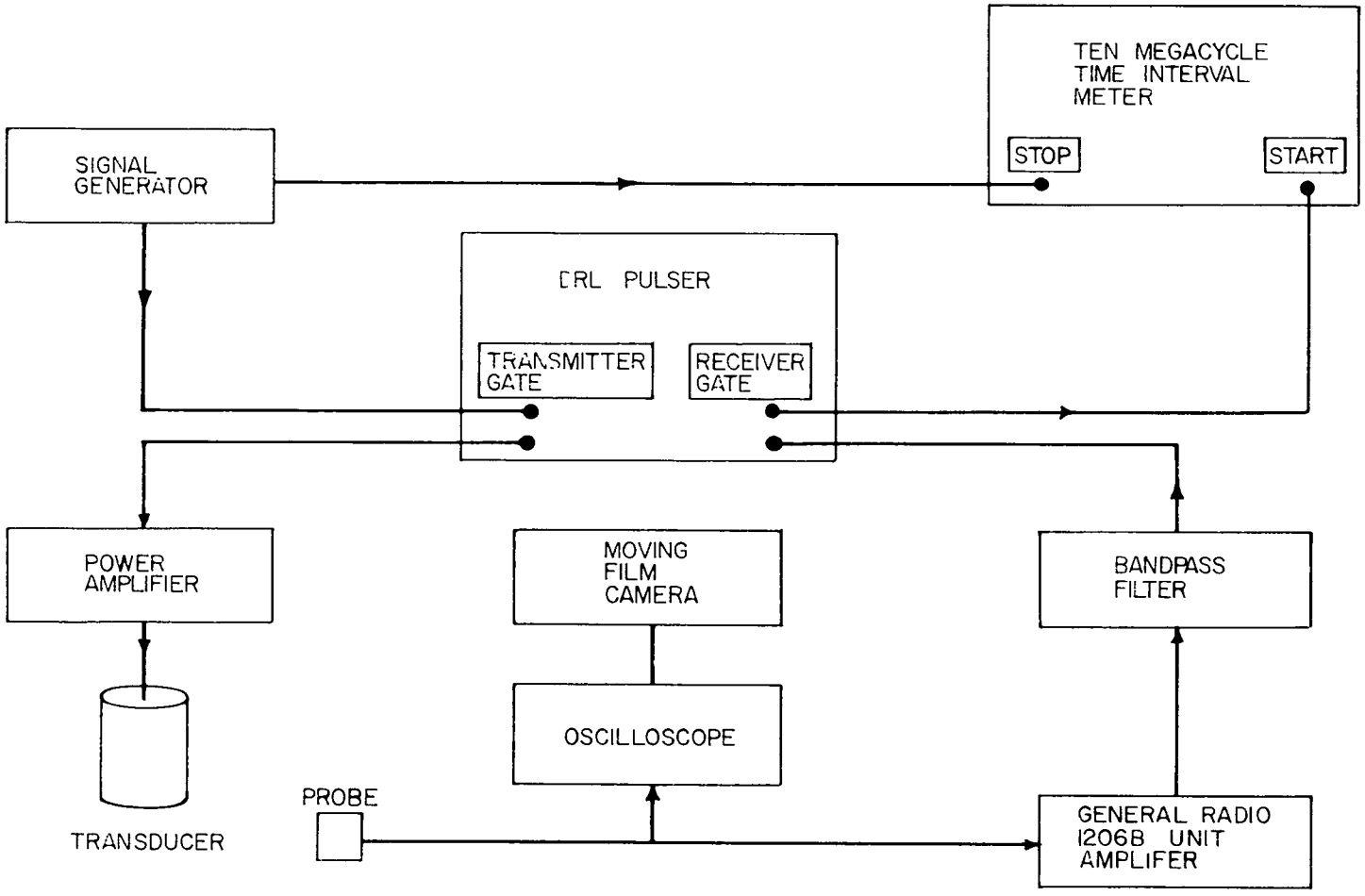

SYSTEM DIAGRAM FOR PULSED TRANSMISSION
NEARFIELD MEASUREMENTS

The pulse received with the probe was displayed on an oscilloscope equipped with a moving-film camera. With the film moving at the proper speed, a photograph was made of each pulse as it was received. By the use of a film reader, the amplitudes of the center portions of the pulses were measured.

For phase measurements a 10-Mc time interval meter was used. Because the minimum signal for triggering the meter was about 0.5 volt rms, amplification to high voltage levels was necessary in order to measure phase over a dynamic range of 30-40 db. A General Radio Unit Amplifier was used for this amplification with a bandpass filter for improving the signal-to-noise ratio. If the maximum signal from the probe had been less than approximately 0.5 volt rms, it would have been necessary to use additional voltage amplification ahead of the unit amplifier. In order to measure phase in this same center portion of the pulses, the amplified signal was gated through the receiver gate of the DRL pulser. This gate is synchronized with the transmitter gate and was adjusted to open at the time the center portion of the pulse was received. The output of this gate was applied to the start input of the time interval meter. This input was adjusted to trigger the meter when the voltage crossed the zero axis going from negative to positive. This made the triggering relatively insensitive to level changes. The signal from the signal generator was applied to the stop input of the time interval meter. For each pulse received the meter read a value of relative phase in units of 10^{-7} seconds. To obtain phase in radians these readings would have been multiplied by 2π and divided by the period of the signal in 10^{-7} seconds. It was possible to log these "phase" readings by hand because of the slow pulse rate used. Ideally, a printer would be used to do this automatically.

In farfield measurements only the oscilloscope and camera were necessary for measuring the amplitude.

Freefield Procedure

With freefield conditions available, the probe or line was placed in the nearfield on the freefield side and the transducer was rotated. As stated previously, the rotation mechanism triggered the pulser each 3.6 degrees of

rotation. Pulselengths used were sufficiently long for steady-state conditions to be reached. The amplitudes were recorded on film automatically, and the phases were recorded by hand.

In farfield measurements the hydrophone was placed sufficiently far away on the freefield side, and the procedure was repeated without measuring the phase.

Tank Procedure

When measurements were made in the tank, farfield measurements were not possible and nearfield measurements were carried out in much the same way that they were in the freefield. Great care was taken, however, to make the measurements after steady-state conditions were reached but before reflections from the tank walls had reached the probe. This involved placing the transducer on one side of the tank and placing the probe near the center of the tank in order to have the probe as far from the tank wall as possible (see Chapter III).

Proposed System

The original pulsed-transmission measurement system will soon be modified to make it more reliable and versatile. The principal addition to it is a digital voltmeter capable of measuring the amplitude of a short pulse. The time required for making this measurement is only about two periods of the signal used. This will mean that amplitude and phase can both be measured quite rapidly, and the readings will be available in digital form for applying to a printer. The printer will record amplitude and phase readings on the same line of a paper tape. This will eliminate some chances of human error. A digital-to-analog converter and an X-Y recorder will also be added to the system. These will make it possible to plot amplitude or phase versus position directly as the measurements are made.

The new system will be compatible with a paper tape punch for recording data if this is ever necessary. Another digital-to-analog converter and X-Y recorder may also be added if it becomes necessary to make analog plots of amplitude and phase simultaneously.

15 March 1962
DDB/lb

CHAPTER III

MEASUREMENTS WITH FOUR TYPES OF TRANSDUCERS

Introduction

In order to check the theory of the computation of farfield directivity patterns and source levels, preliminary nearfield measurements were made on four types of transducers. Computations were made and agreed well with measured values.

Details of the measurements and computations are presented in this chapter, as are the computed farfield patterns. They are compared with equivalent measured patterns.

Line Transducer

The line transducer is shown in Dwg. AS-4911. The dots along the outline indicate points at which nearfield data were taken. Since the transducer is very nearly omnidirectional in a plane normal to the axis, it was assumed to be omnidirectional. Thus the probe, which was much less than a wavelength from the surface of the transducer, was moved along the line at only one azimuth as shown in Dwg. AS-6577. It was moved by the use of a lead-screw mechanism with a position indicator. The transducer was driven continuously, and data were recorded at only the twelve points indicated.

The surface of integration was a cylinder of approximately the same length as the transducer. Due to the omnidirectionality assumption, the integration around the axis was performed analytically. This reduced the problem to the numerical evaluation of a line integral.

A farfield pattern in a plane which contains the axis of the line was computed on a digital computer The points are seen in Dwg. AS-4911 as compared with the equivalent measured pattern.

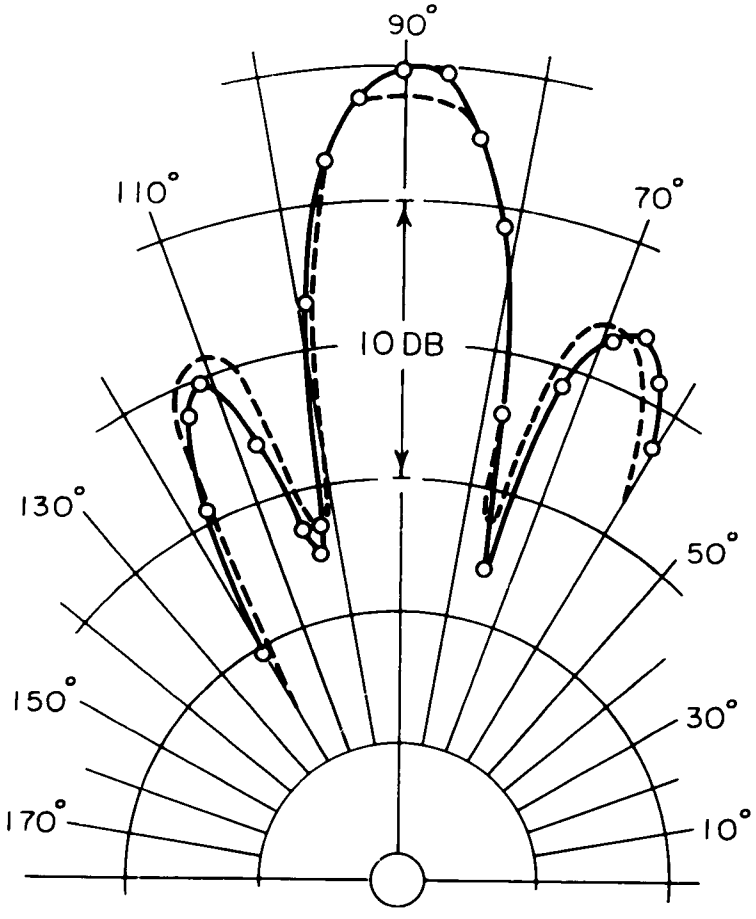

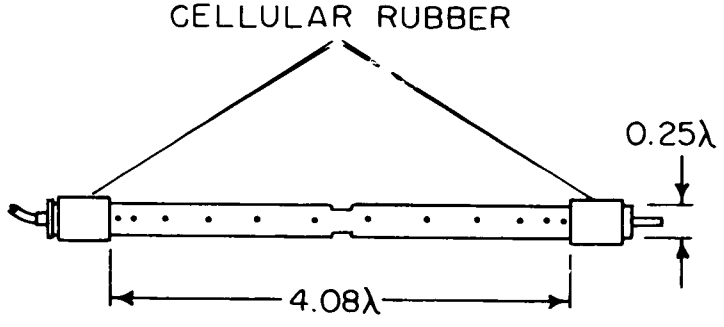

LINE HYDROPHONE OUTLINE AND FARFIELD PATTERNS

DRL – UT
DWG A S 4
GSI – CL
5 – 27 – 6

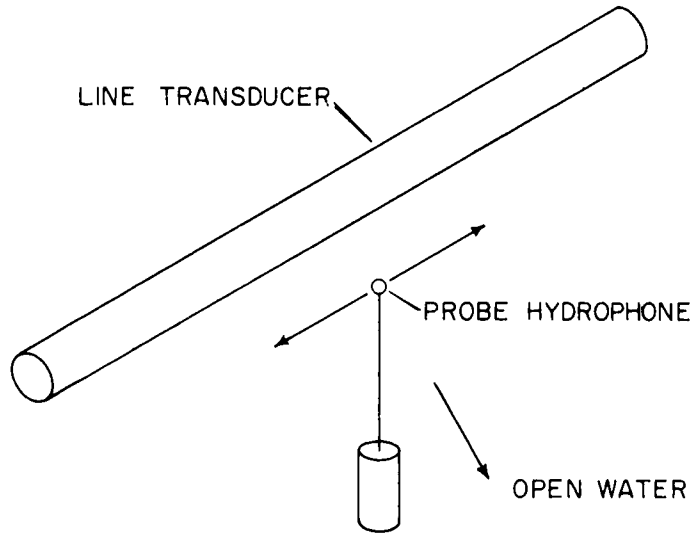

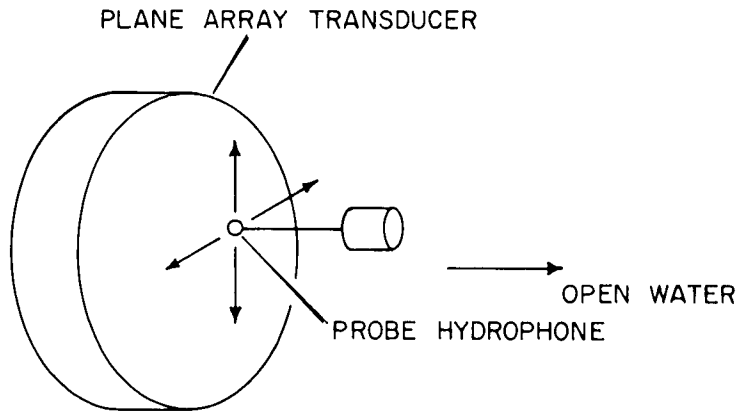

LINE AND PLANE ARRAY TRANSDUCER LAYOUT

DRL - UT
DWG AS 6577
DDB - LFH
3 - 2 - 62

Plane Array Transducer

The diagram of the plane array transducer shown in Dwg. AS-4913 is an outline of the active face. Continuous-transmission data were taken at points on a plane one-third of a wavelength in front of the active face as previously shown in Dwg. AS-3577. The locations of the points are indicated by the dots on the diagram in Dwg. AS-4913. Probe positioning was accomplished by moving the lead-screw device in this plane.

The surface of integration was a square portion of a plane which extended across the active face as shown in the diagram. A farfield directivity pattern in a plane normal to the plane of the array was computed and is compared with an equivalent measured pattern in Dwg. AS-4913. The integration was again performed numerically on a digital computer.

Dipole Transducer[6]

The dipole transducer was a square, plane array which measured 0.27 wavelength on the side and 0.09 wavelength in thickness. The active faces were the two square sides. The outline in Dwg. AS-4912 shows the edge view of the transducer. Drawing AS-6578 shows another view with the probe in position. The transducer was driven continuously, and amplitude and phase were recorded continuously around the transducer. Data were read from the recordings at points which correspond to the dots on the diagram in Dwg. AS-4912. Measurements were made in three planes parallel to the plane of the diagram. This was done by making three passes around the transducer with a probe. In addition, a line hydrophone was used to make another set of nearfield measurements.

The surface of integration was a cylinder which extended in length only slightly beyond the transducer. Farfield patterns in the plane of the diagram were computed for each of the sets of data. Results of the computations were very similar. The computed points from the three-level data are shown compared with a measured pattern in Dwg. AS-4912.

---

[6] G. S. Innis and C. W. Horton, Defense Research Laboratory Acoustical Report No. 172. Contract NObsr-72627, June 1960 (CONFIDENTIAL).

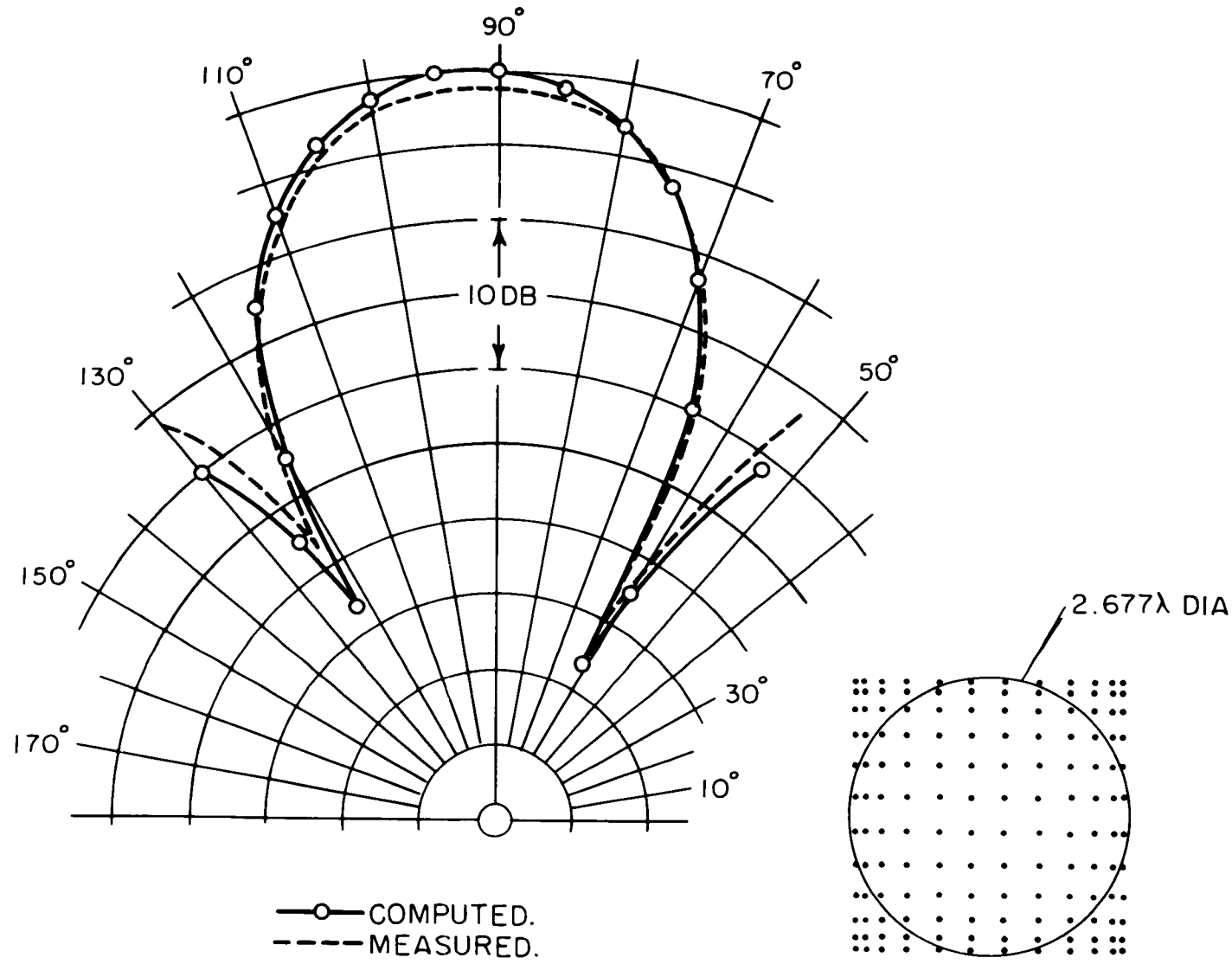

DRL – UT
DWG AS 4913
GSI – CLW
5–27–60

PLANE ARRAY OUTLINE AND FARFIELD PATTERNS

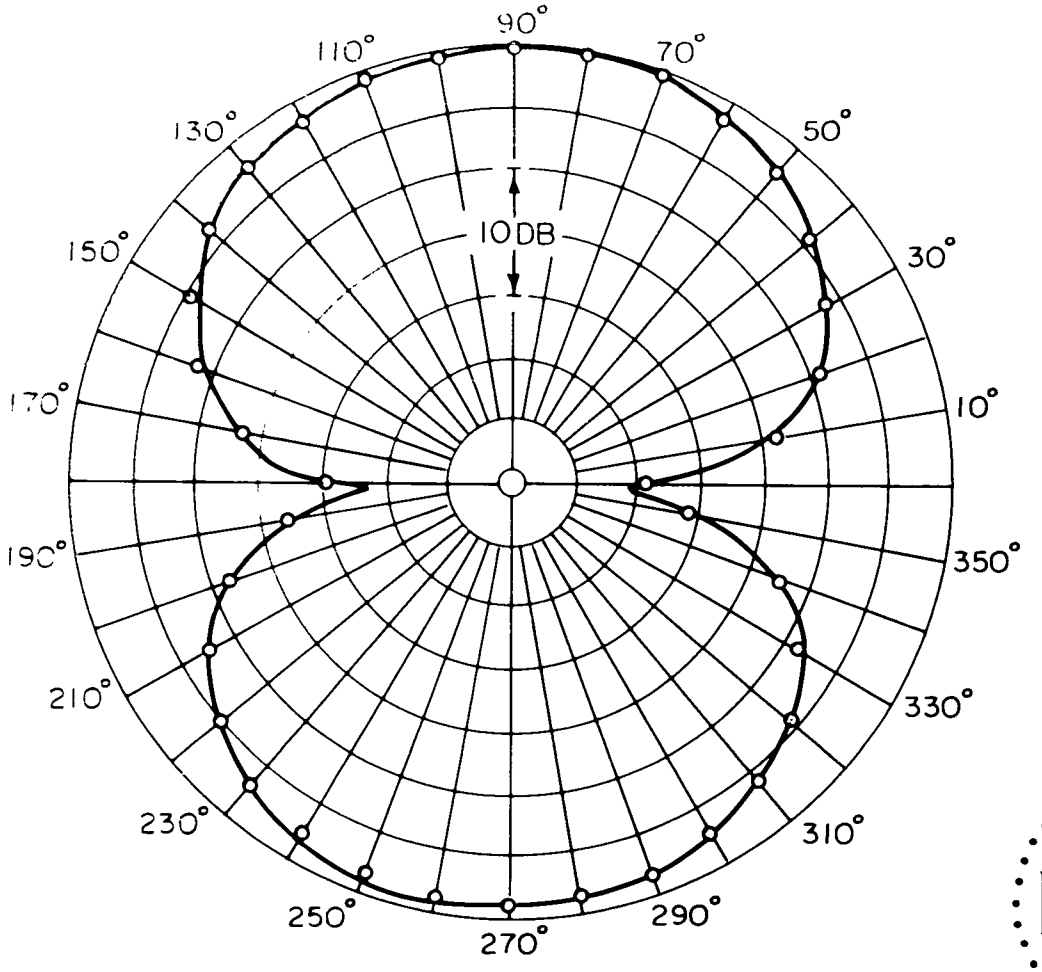

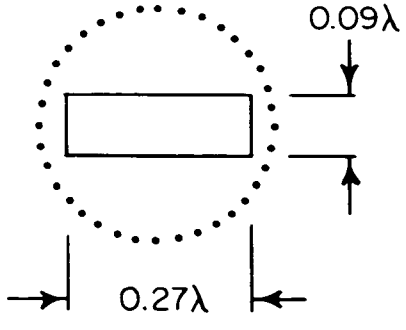

o COMPUTED.
—— MEASURED.

DIPOLE RADIATOR OUTLINE AND FARFIELD PATTERNS

DRL - UT
DWG. A5 4
GS1 - COM
5 - 27 - C

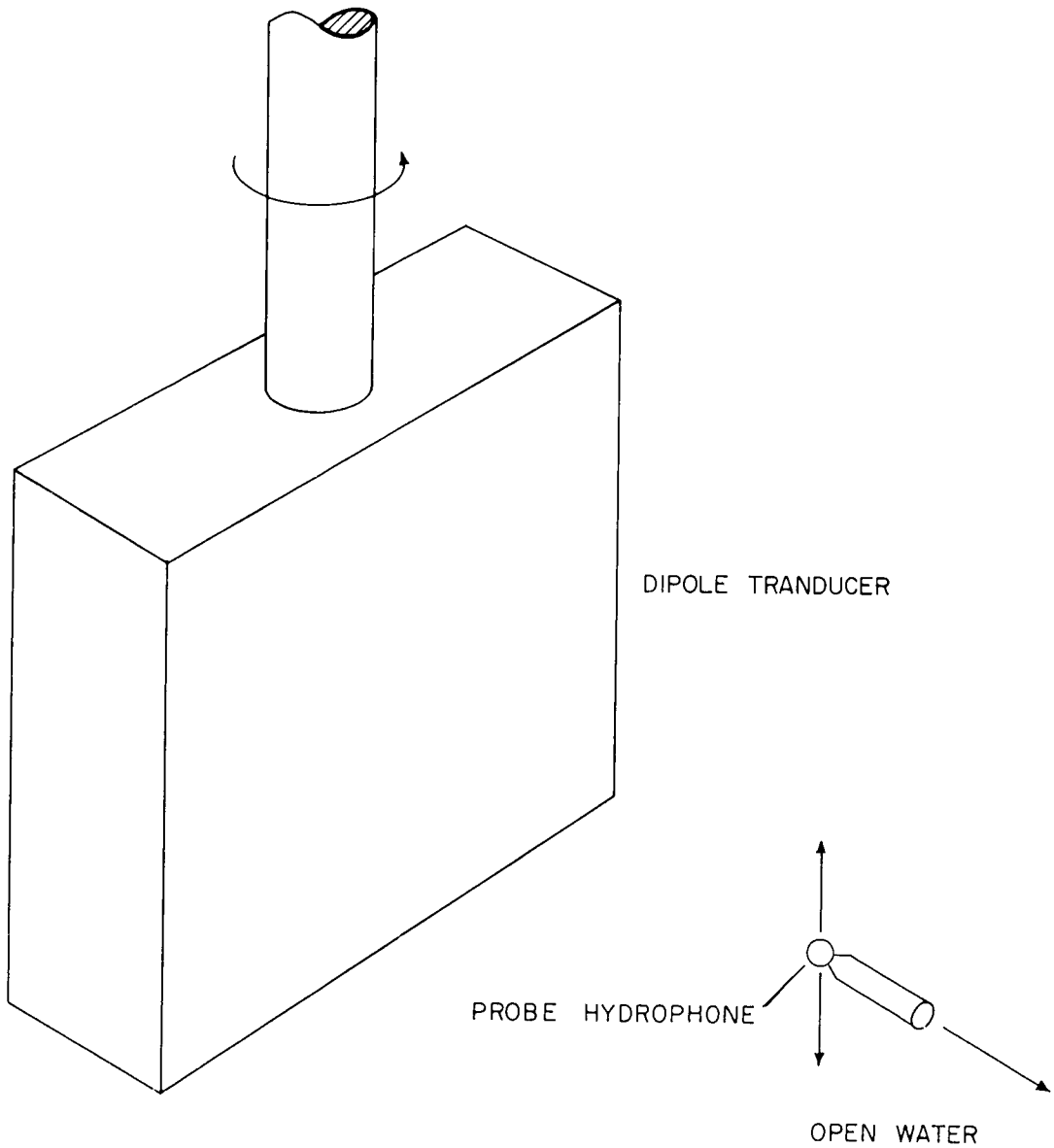

DIPOLE TRANSDUCER LAYOUT

Line-and-Cone Transducer

A diagram of the line-and-cone transducer is shown in Dwg. AS-6496. This transducer consists of a 90° conical reflector with an 18" aperture. Along the conical axis is mounted a 9", 16-element line transducer. Measurements were made on a plane just in front of the aperture. Continuous recordings of amplitude and phase were made as the probe was moved from a point along the conical axis outward for 12" along a line perpendicular to the axis. The transducer and probe arrangement is shown in Photo 72627-223. Data were taken from the recordings at various increments, depending upon the frequency of operation and the configuration of the elements of the transducer. Measurements were made at several frequencies from 15 to 100 kc with several element configurations.[7]

The surface of integration was a circular portion of a plane. Symmetry about the axis of the cone was assumed in the computer program. Points of a computed pattern in a plane containing the conical axis are compared with a measured farfield pattern in Dwg. AS-6496. The patterns illustrated are for 15 kc with all of the transducer elements in parallel. Patterns were computed for several frequencies and element configurations with about the same success.

Conclusions

Agreement between measured and computed patterns was generally good. The line and plane array patterns were slightly too broad, because the measurements and integrations were carried out only across the active faces. Because this procedure neglects small pressures beyond the active face, it approximates the source by a slightly smaller source. This results in patterns which are slightly too broad. If the surfaces of integration had been extended somewhat, the computed patterns might have been the correct width. It is possible, however, to extend these surfaces to a point where computed patterns are too narrow. Generally, it is satisfactory to integrate only across the active face and to tolerate the slight pattern broadening.

---

[7] D. L. Baird, An Experimental Investigation of an Underwater Sound Transducer-Reflector Combination, Master's Thesis, The University of Texas, January 1962.

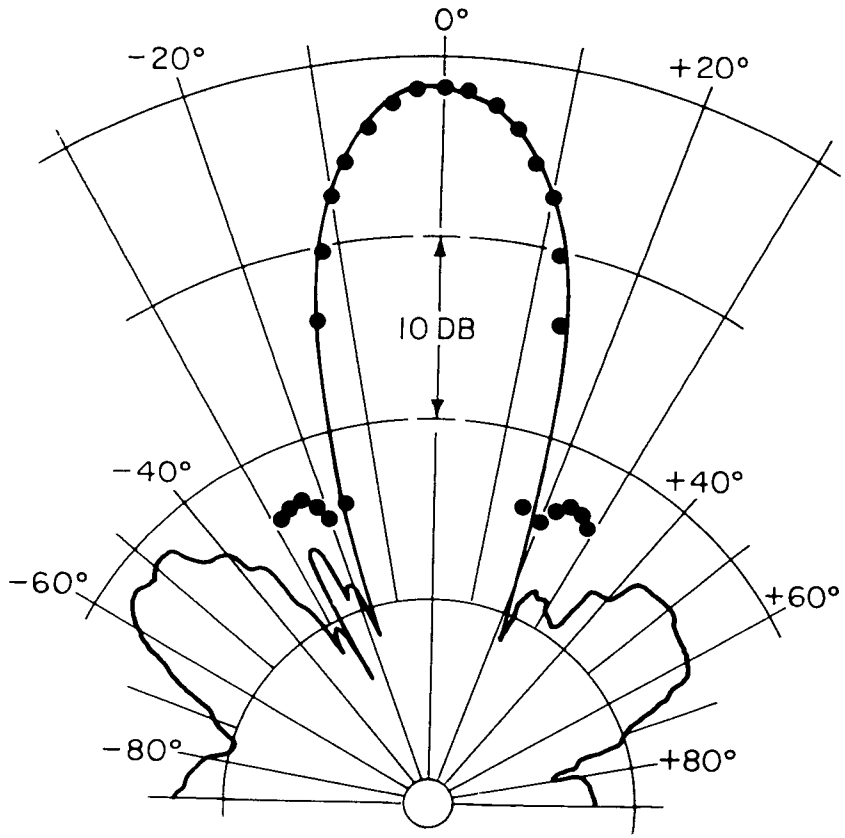

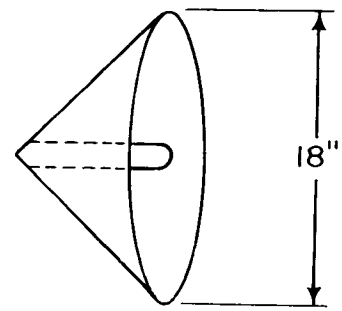

● COMPUTED POINTS
— MEASURED PATTERN

DRL – UT
DWG A3 6496
DDB – EJW
1 – 25 – 62

LINE-AND-CONE DIAGRAM AND FARFIELD PATTERNS AT 15 KC

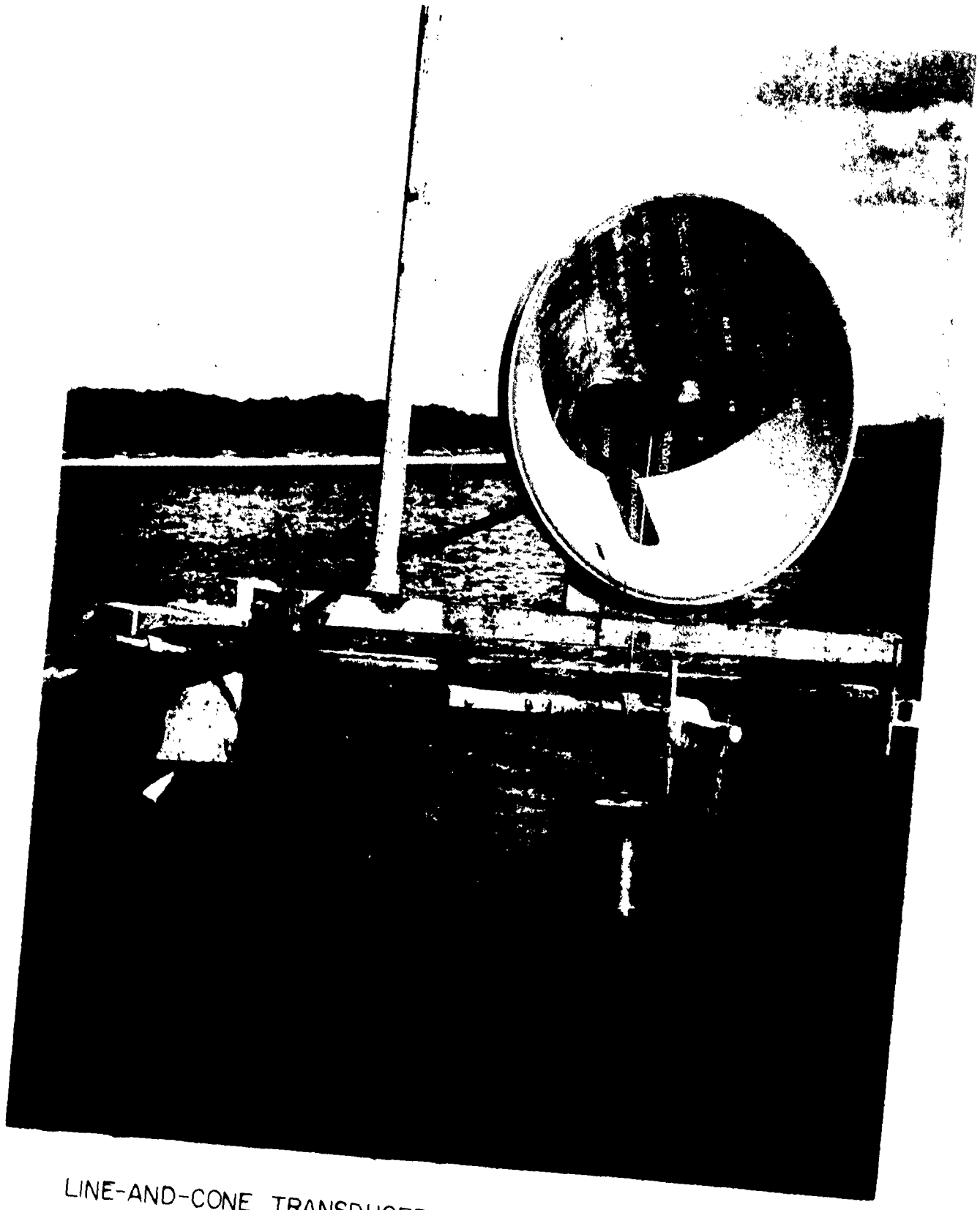

LINE-AND-CONE TRANSDUCER AND PROBE ARRANGEMENT

The agreement between measured and computed patterns and source levels was excellent in the case of the dipole. The pattern agreement in the line-and-cone case was very good in the major lobe region.

It is doubtful that the approximation of ikp for the normal component of the pressure gradient caused any inaccuracies in these cases. The validity of the approximation was more doubtful in the dipole case; this was because the surface of integration did not fit the transducer very closely and the pressure varied over the surface as much as 20 db during a probe travel of 0.05λ. In spite of this, agreement between computed and measured patterns was excellent.

C H A P T E R I V

MEASUREMENTS WITH A LARGE CYLINDRICAL TRANSDUCER

Introduction

Extensive nearfield measurements and computations were made on an AN/SQS-4 Mod 3 transducer. Emphasis was placed on this transducer because it was a large, low-frequency ASW transducer, one of the type for which the nearfield calibration techniques are important.

Details of the measurements and computations are presented for both freefield and tank conditions. Computed patterns are compared with measured ones.

Transducer Description

A sketch of the transducer is shown in Dwg. AS-6506. It is built of 48 vertical staves which are equally spaced about its axis. Each of the staves consists of nine magnetostrictive elements along its length. The length of each stave is 25.5 in.; the diameter of the transducer is 33.5 in.

Freefield Measurements

Originally, the transducer was driven continuously and continuous recordings of amplitude and phase were made as described in Chapter II. From the recordings, data were read each 3.6° of transducer rotation. In order to operate near the full power rating of the transducer it was necessary to change to pulsed operation and, consequently, to the other measuring system described in Chapter II. With the transducer transmitting a pulse each 3.6° of rotation, the amplitude and phase of each pulse was recorded. There was little difference observed in the results of continuous and pulsed measurements at various power levels. In the following discussions it will be noted whether the measurements were continuous or pulsed, but this seems to be an insignificant point.

The surface of integration for the farfield computations was a right, circular cylinder 26 in. long and 45.5 in. in diameter. Measurements were

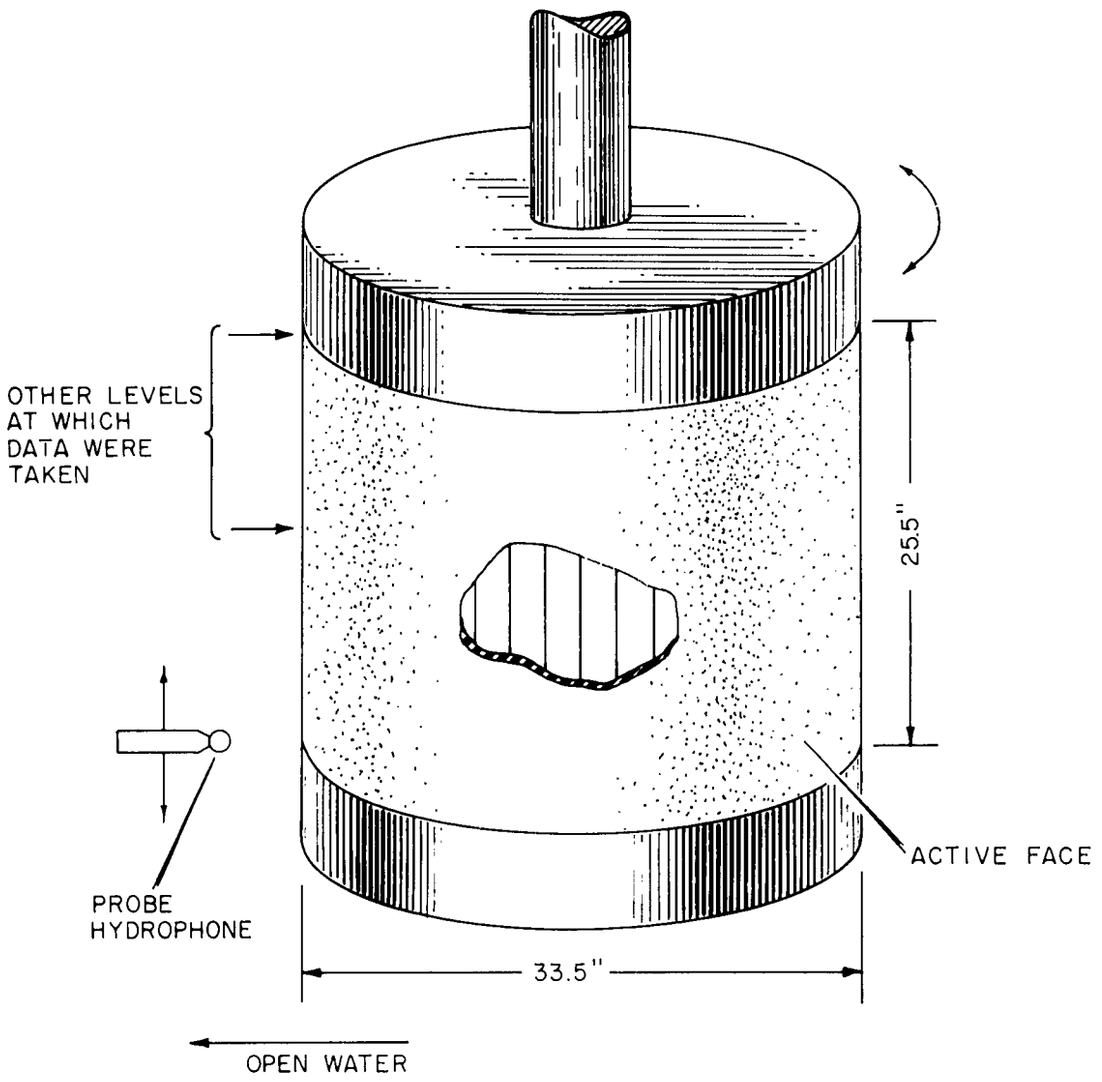

AN/SQS-4 TRANSDUCER LAYOUT

made around the transducer with an Underwater Sound Reference Laboratory type 3A probe at from 1 to 27 vertical levels. In most cases the location of these levels was prescribed by the use of the Gaussian quadrature formula for the vertical integration. The locations of the three levels shown in Dwg. AS-6506 were determined by this method. The transducer was driven with six consecutive staves connected in parallel and with twelve consecutive staves in parallel. Horizontal and vertical farfield patterns were computed on a digital computer.

Drawings AS-5694 and AS-5692 are sample plots of the six-stave nearfield data. The circles represent the 100 values at 3.6° increments that were used in the computations. Drawings AS-5693 and AS-5691 show similar data plots for the twelve-stave case.

Drawing AS-6036 shows two computed patterns compared with the equivalent measured patterns. These were computed from one-level and three-level measurements made while driving six staves continuously. Similar patterns for twelve staves are shown in Dwg. AS-6038, except that the measurements were made at one and four levels. The four-level measurements were made with pulsed transmission.

Because it was desirable to attempt to compute vertical farfield patterns, it was necessary to make a set of measurements at a greater number of vertical levels spaced no farther apart than 0.8λ. Six-stave, continuous-transmission measurements were made at 27 levels, spaced 1 in. apart. Thus there were data from 100 points at each of 27 levels; that is, 2700 amplitudes and 2700 phases. Vertical patterns were to be computed at the azimuth corresponding to the center of the major lobe of the horizontal directivity pattern. In order to avoid a computer storage problem, only 40 of each group of 100 data were used. These were the 40 that were centered about the active face. This meant that the apparently meaningless data in the back region were neglected, and the computer assumed zero pressure in these locations. A vertical pattern, computed by using these data from all 27 levels, is shown in Dwg. AS-6035. Other vertical patterns were computed by using data from fewer levels which

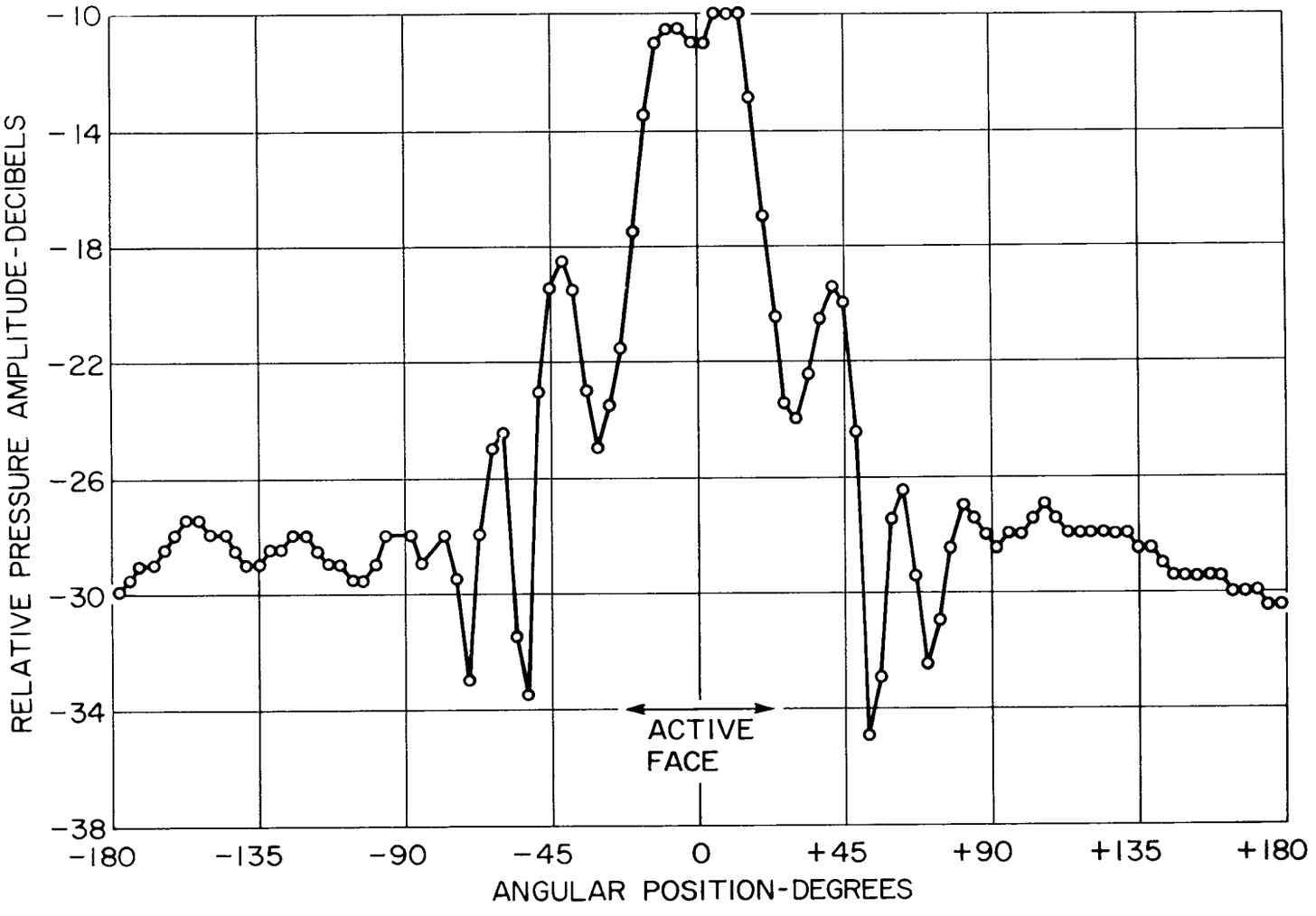

RELATIVE PRESSURE AMPLITUDE VS. ANGULAR POSITION
WITH 6 STAVES OF TRANSDUCER DRIVEN CONTINUOUSLY

RADIAL PROBE POSITION: 6.0" FROM ACTIVE FACE

VERTICAL " " : 24.8" BELOW TOP OF ACTIVE FACE

ORL - UT
DWG A S564
DDB - EJW
4 - 28 - 61

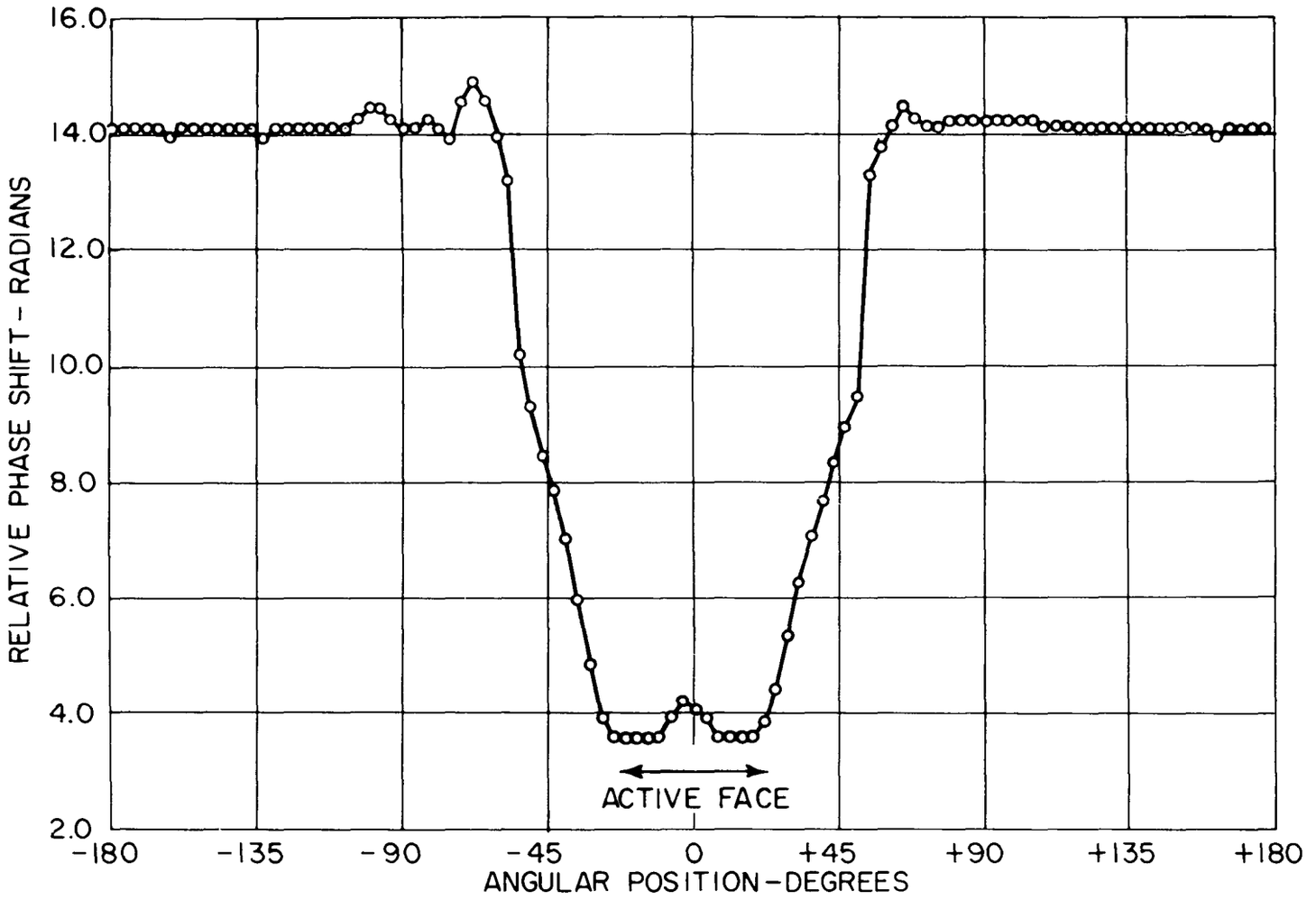

DRL - UT
DWG AS 5692
DDB - LRS
4 - 28 - 61

RELATIVE PHASE SHIFT VS ANGULAR POSITION WITH
6 STAVES OF TRANSDUCER DRIVEN CONTINUOUSLY

RADIAL PROBE POSITION : 6.0" FROM ACTIVE FACE
VERTICAL " " : 24.8" BELOW TOP OF ACTIVE FACE

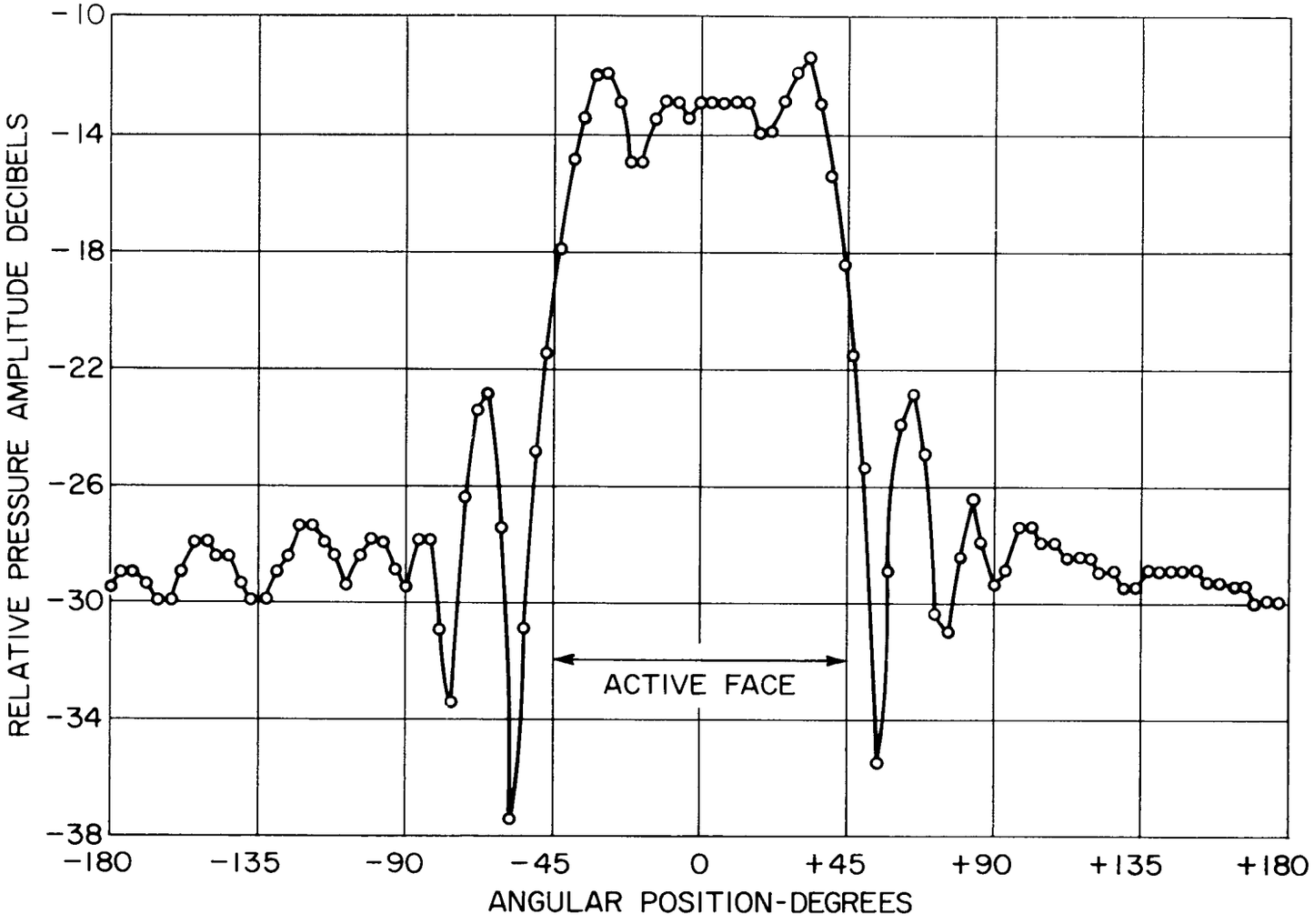

RELATIVE PRESSURE AMPLITUDE VS. ANGULAR POSITION
WITH 12 STAVES OF TRANSDUCER DRIVEN CONTINUOUSLY

RADIAL PROBE POSITION: 6.0" FROM ACTIVE FACE
VERTICAL " " : OPPOSITE CENTER OF ACTIVE FACE

DRL - UT
DWG AS 5693
DDB - EJW
4 - 28 - 61

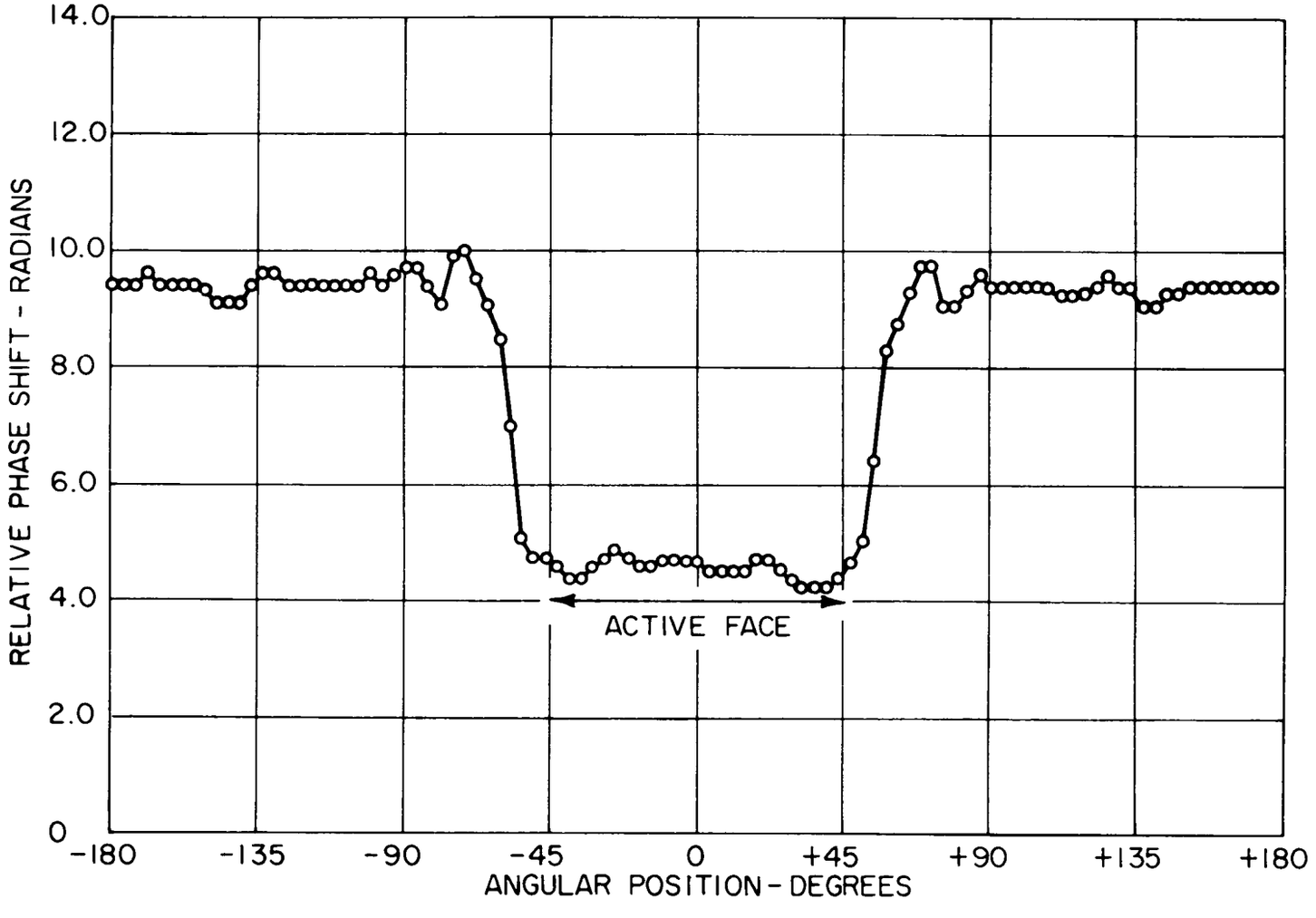

DRL - UT
DWG AS 5691
DDB - LRS
4-28-61

RELATIVE PHASE SHIFT VS ANGULAR POSITION WITH
12 STAVES OF TRANSDUCER DRIVEN CONTINUOUSLY

RADIAL PROBE POSITION: 6.0" FROM ACTIVE FACE
VERTICAL " " : OPPOSITE CENTER OF ACTIVE FACE

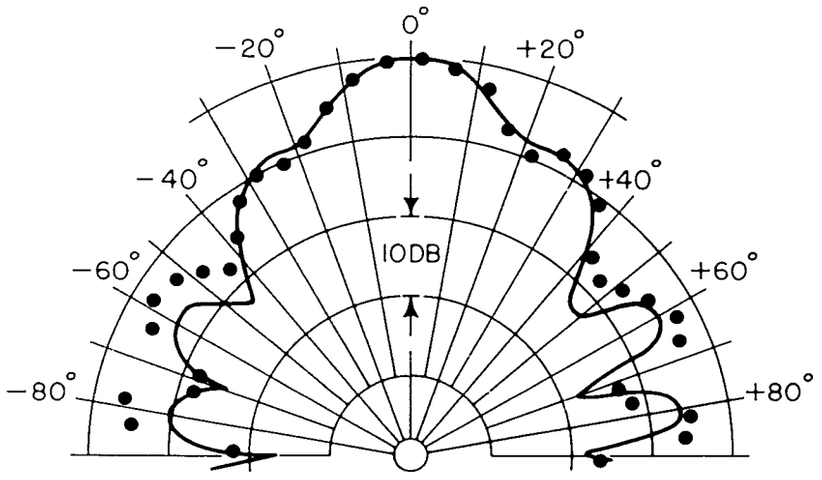

FROM DATA TAKEN
AT 1 LEVEL

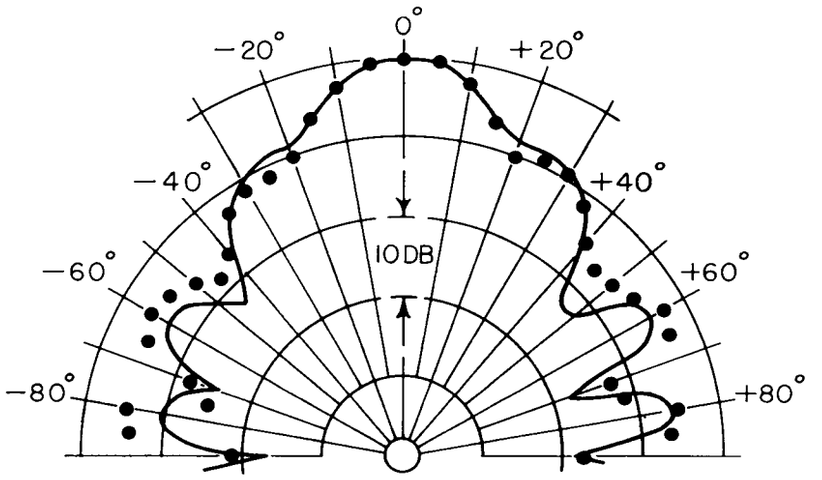

FROM DATA TAKEN
AT 3 LEVELS

• COMPUTED POINTS
— MEASURED PATTERN

HORIZONTAL FARFIELD DIRECTIVITY PATTERNS DRIVING 6 STAVES

DRL – UT
DWG AS6036
DDB – PPR
9 – 12 – 61

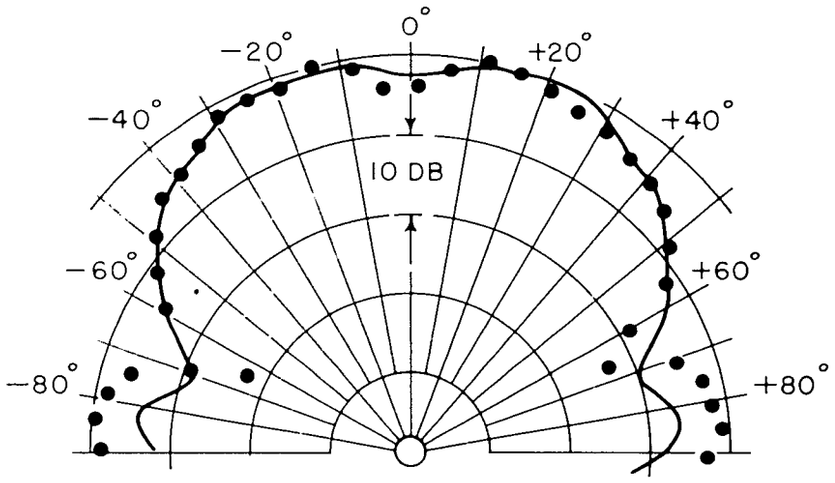

FROM DATA TAKEN
AT 1 LEVEL

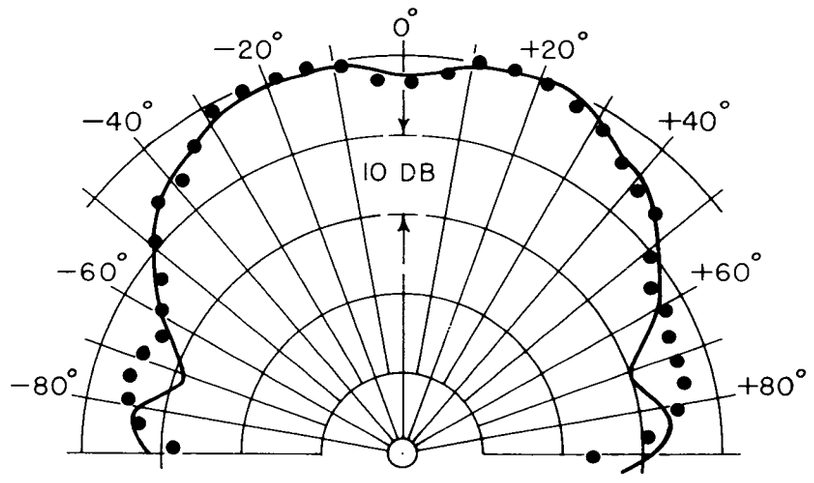

FROM DATA TAKEN
AT 4 LEVELS

● COMPUTED POINTS
— MEASURED PATTERN

HORIZONTAL FARFIELD DIRECTIVITY PATTERNS DRIVING 12 STAVES

ORL – UT
DWG AS6038
DDB – PPR
9 – 14 – 61

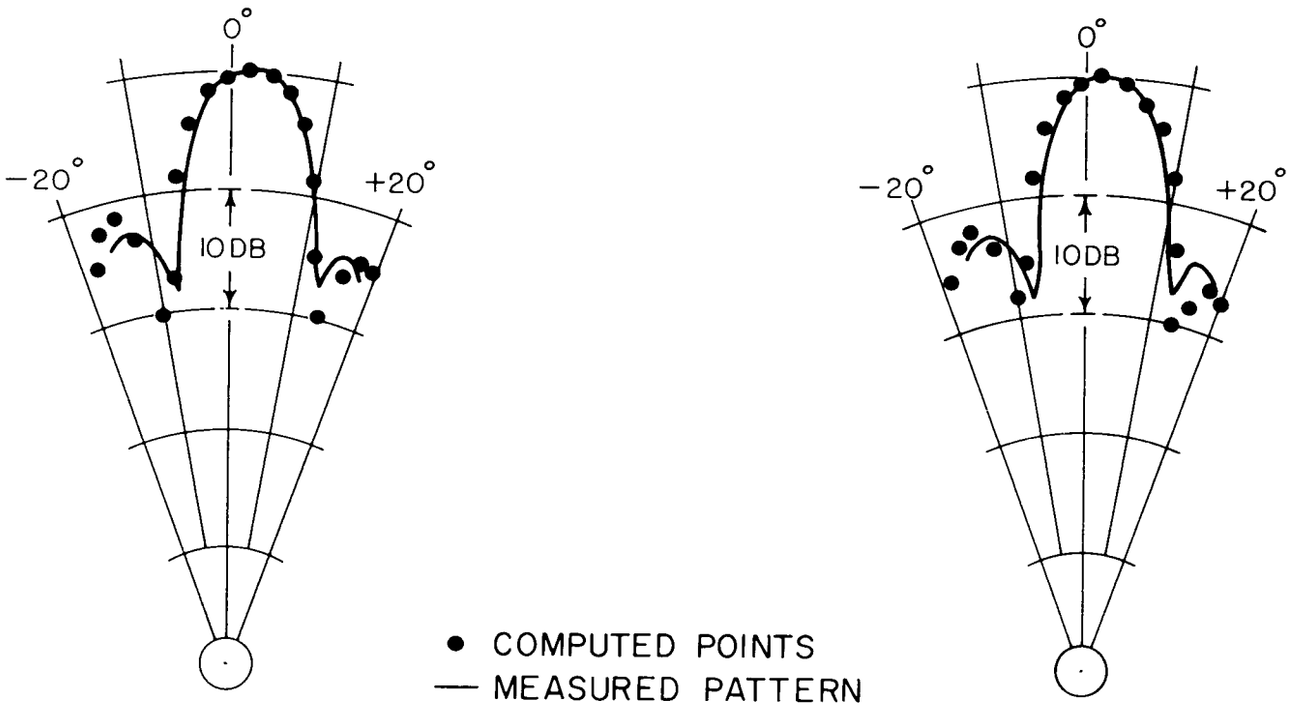

FROM DATA TAKEN
AT 27 LEVELS

FROM DATA TAKEN
AT 11 LEVELS

VERTICAL FARFIELD DIRECTIVITY PATTERNS DRIVING 6 STAVES

were selected from the entire set. Also shown in Dwg. AS-6035 is a pattern computed with data from 11 levels spaced to fit the Gaussian quadrature formula. Drawing AS-6037 shows a horizontal pattern computed from the 27 x 40 array of data described above.

Measurements for computing horizontal patterns were also made by the use of a 33-in. SKH line hydrophone. Pulsed nearfield measurements were made around the transducer at 100 points, as previously. Computations were carried out as before except that the surface of integration was longer due to the length of the line hydrophone.

Drawing AS-6037 also shows a pattern computed from line hydrophone data taken while driving six staves. Drawing AS-6039 shows the same type of pattern for the twelve-stave case.

In three of the measurements described previously, the line or probe hydrophone was calibrated, and the source level of the transducer was computed. These values agreed with values measured in the farfield to within ±1 db in all of the cases.

Tank Measurements

The layout of the cylindrical transducer in the tank is shown in Dwg. AS-6457. It was decided to attempt to make pulsed measurements in the same way as was done previously, exercising great care to measure near the leading edge of the received pulse. This would hopefully allow the measurement to be completed before energy reflected from the tank walls had time to propagate to the hydrophone. However, the transducer has an appreciable risetime which must elapse at the start of a pulse before steady-state conditions are reached. Received pulses of various pulse lengths are shown in Dwg. AS-6521. It can be seen that the steady-state had essentially been reached after 1.0 msec. It can also be seen that the direct and reflected pulses were resolved up to pulse lengths of about 1.5 msec. At greater pulse lengths the leading 1.5 msec portion of the direct pulse was clean, but the remainder of it was partially cancelled by the reflected pulse. It might

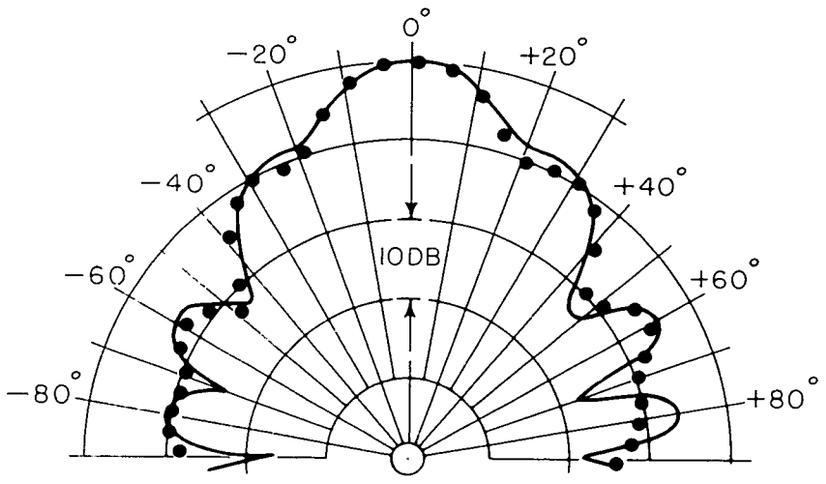

FROM DATA TAKEN
AT 27 LEVELS

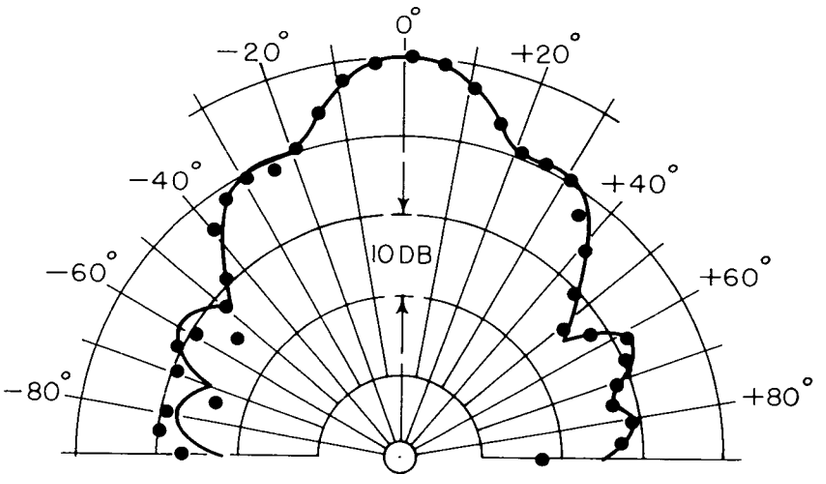

FROM DATA TAKEN WITH
LINE HYDROPHONE

• COMPUTED POINTS
— MEASURED PATTERN

HORIZONTAL FARFIELD DIRECTIVITY PATTERNS DRIVING 6 STAVES

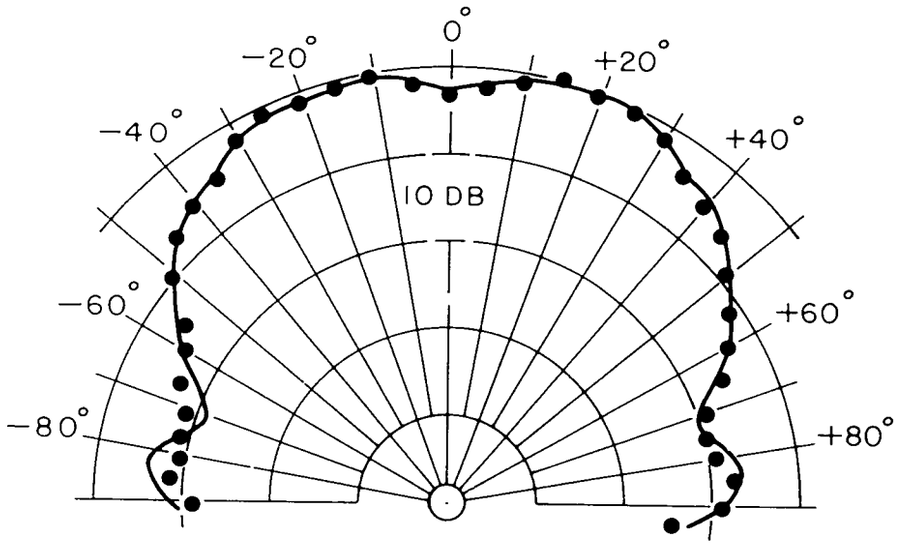

● COMPUTED POINTS
— MEASURED PATTERN

FROM DATA TAKEN WITH
LINE HYDROPHONE

HORIZONTAL FARFIELD DIRECTIVITY PATTERN DRIVING 12 STAVES

DRL – UT
DWG AS 6039
DDB – PPR
9 – 14 – 61

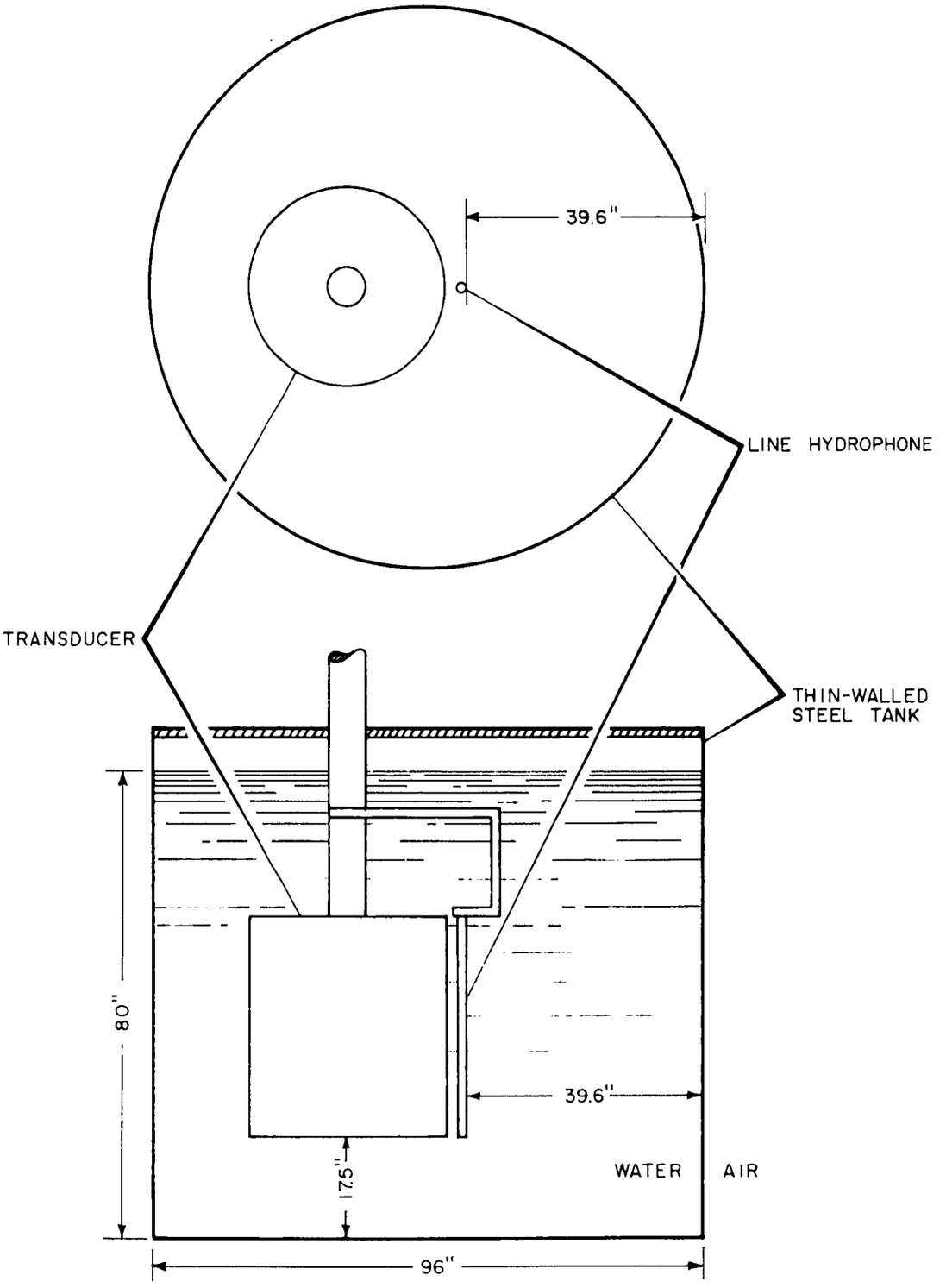

LAYOUT OF CALIBRATION TANK

DRL - UT
DWG AS6457
DDB - LRS
1 - 25 - 62

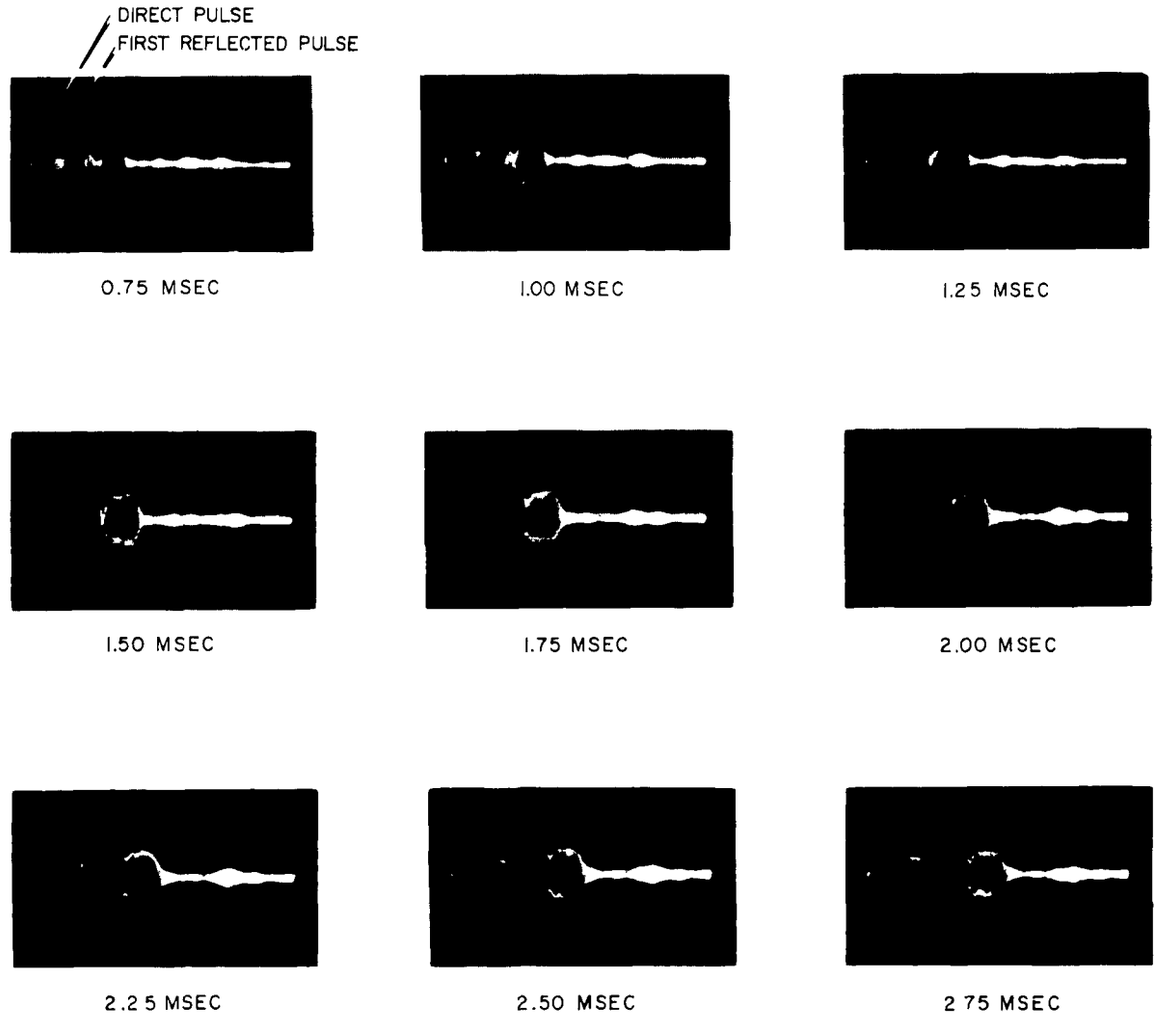

SIGNAL RECEIVED IN TANK TRANSMITTING
AT VARIOUS PULSE LENGTHS

DRL – UT
DWG AS 6521
DDB – PPR
2 – 2 – 62

be said that the transducer was in freefield conditions for a duration of 1.5 msec. Since the steady-state had been reached after 1.0 msec, there still remained 0.5 msec in which to make the measurement. This was easily done by the procedures described earlier.

The data were obtained with the line hydrophone at distances from the transducer of 0.42 and 0.84λ. Again there were 100 data obtained for the six-stave and twelve-stave cases. The computations were carried out as they had been previously. In Dwgs. AS-6458 and AS-6459 the computed patterns are compared with farfield patterns which were measured before the transducer was placed in the tank. In all four of the cases, computed source levels were within ±1 db of previously measured ones.

Conclusions

Results from the original probe measurements at a few vertical levels were considered to be quite useful, although not perfect. It was quite surprising that the computed patterns from three-level data were not appreciably better than those from one-level data. It would seem that better sampling of the pressure over the surface would yield truer results. At this point most of the blame for pattern inaccuracies fell on the approximation for the normal component of the pressure gradient.

Poor sampling, however, was found to be the cause of the inaccuracies since the improvement in sampling afforded by the use of 27-level data resulted in a great improvement in computed pattern accuracy. The fact that computed patterns from three-level data were no more accurate than those from one-level data can probably be attributed to poor choices of levels. Nevertheless, no better way of choosing levels is known at present.

The improved patterns from the 27-level data were motivation for making measurements with the SKH line hydrophone to see whether further improvement in agreement between measured and computed patterns could be obtained. It can be seen from the drawings that the agreement was improved even more by

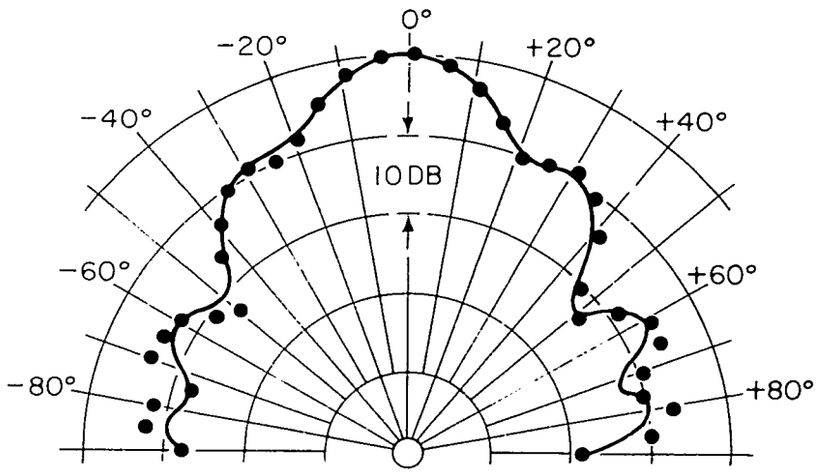

LINE HYDROPHONE AT 0.42λ

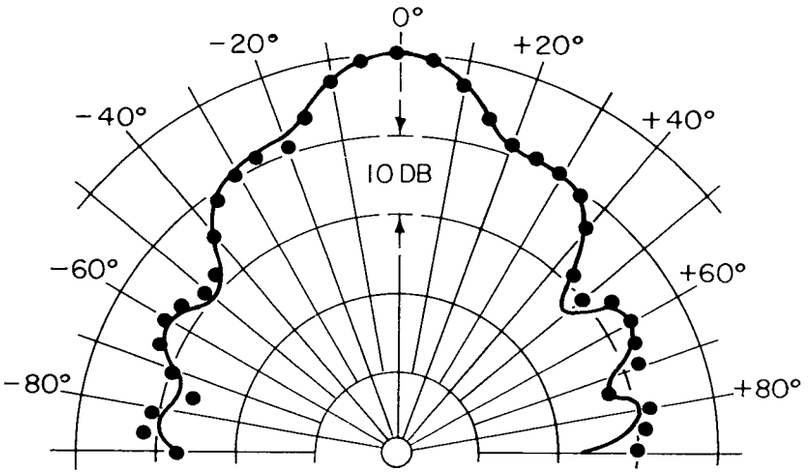

LINE HYDROPHONE AT 0.84λ

• COMPUTED POINTS
— MEASURED PATTERN

HORIZONTAL FARFIELD DIRECTIVITY PATTERNS DRIVING 6 STAVES

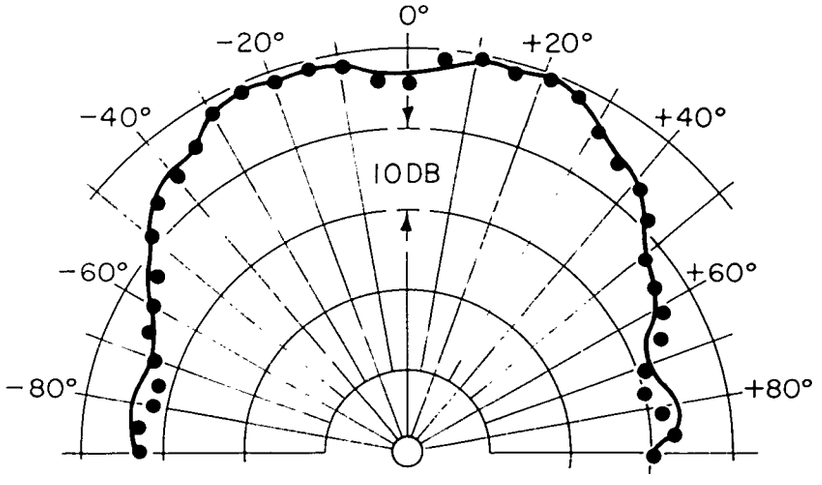

LINE HYDROPHONE AT 0.42 λ

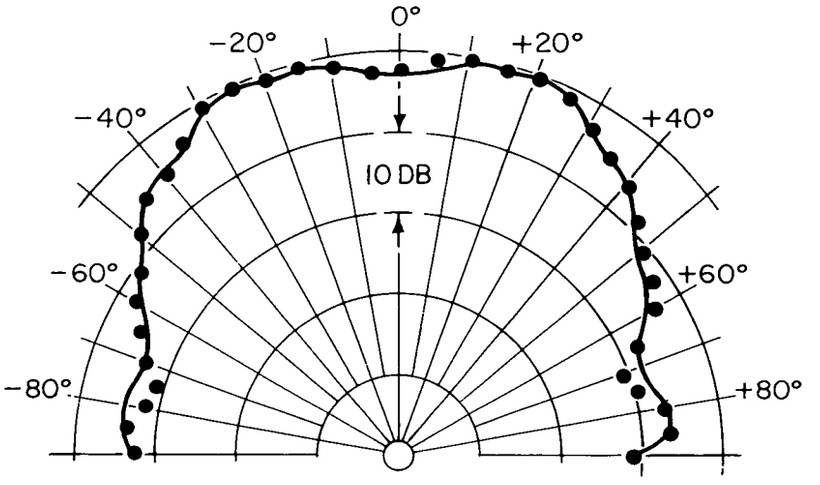

LINE HYDROPHONE AT 0.84 λ

• COMPUTED POINTS
— MEASURED PATTERN

HORIZONTAL FARFIELD DIRECTIVITY PATTERNS DRIVING 12 STAVES

ORL - UT
DWG AS 6459
DDB - EJW
1 - 25 - 62

the use of the line hydrophone. Also, if only horizontal patterns were desired, a set of line-hydrophone data could be obtained in minutes, where a set of 27-level data would probably take the better part of two days.

The computed vertical patterns agreed well with the measured ones in shape but the major lobes were slightly too broad. This is not a surprising result when it is considered that the surface of integration was only about as long as the active face. There were surely non-zero pressures beyond the ends of the surface. Neglecting such pressures has an appreciable broadening effect on computed vertical patterns but has very little effect on horizontal patterns. Extending the surface in length might have improved the width of the computed vertical pattern. Generally, it is satisfactory to integrate only across the active face and to tolerate the slight pattern broadening.

It is significant that in several cases the full set of 100 data was not used. Evidently, neglecting the back-region data (pressures which were down only about 20 db) had little or no effect upon pattern accuracy. Such a result as this can only be obtained empirically for a given transducer.

The approximation for the normal gradient of the pressure, which was doubted at the outset, has been shown to be valid for this particular transducer. No way to predict whether the approximation is valid for other cases is known at this time.

The results of the tank measurements described in this report are as good as the results of the equivalent freefield computations. This will always be true as long as it is possible to make steady-state measurements prior to the arrival of reflected energy. The amount of reflecting or absorbing material present in the tank makes no difference. The criterion is that the time it takes the outgoing wave to propagate from the hydrophone to the tank wall and back to the hydrophone must be appreciably longer than the risetime of the transmitted pulse. "Appreciably longer" here may be defined as longer by about two periods of the transmitted frequency. If this criterion is not met, the leading-edge pulse technique cannot be used directly.

In such a situation it will be necessary to take one of two possible approaches. One of these is to make the measurements before the steady-state condition is reached. These measurements could probably be used to compute accurate farfield patterns. However, they would give computed source levels that are all too low by a constant amount. It is probable that the necessary correction for the source levels could be determined from the risetime curve of the transducer. The other possibility is to line the tank with absorbent material to reduce the reflections to a point at which they would cause no appreciable interference. Neither of these two techniques has been tried, but each of them shows promise.

Nevertheless, it is significant that good results have been obtained from nearfield measurements made in a tank that was only about 2.9 times the diameter of the transducer.

15 March 1962
DDB/lb

C H A P T E R V

PRACTICAL SUGGESTIONS FOR SUCCESSFUL NEARFIELD MEASUREMENTS AND COMPUTATIONS

Introduction

The following practical suggestions are presented as the most important points to follow when using nearfield techniques. These points are all covered elsewhere in the report, but are assembled here as a quick-reference check list. More detail on these points can be found in the previous chapters.

General

1. The closed surface of integration should be chosen to fit the shape of the active face of the transducer as closely as possible.

2. Amplitude and phase measurements need not be made over regions of the surface in which amplitudes are down more than 20 to 30 db below the maximum values. The surface can actually be an open surface such as a portion of a plane or the lateral surface of a cylinder.

3. Successful measurements have been made with the probe or line hydrophone at distances from the transducer of 0.25λ to 1.5λ.

4. For accurate source level computations, the probe or line must be calibrated. This should be a standard farfield calibration.

5. Steps should be taken to avoid or to compensate for backlash in the mechanical system. It is important that measurements be made at the points where they are desired.

6. The method of farfield computations has not been tried with cavitation present, and therefore should not be trusted when cavitation occurs.

Probe Measurements

1. If a probe hydrophone is used to measure over the surface, the dimensions of the active face and the overall dimensions perpendicular to the direction of propagation should be 0.25λ or less.

2. In the plane of the pattern to be computed, successive measurement points with the probe should be separated by no more than 0.5λ -- preferably

by no more than 0.5λ. This rule should also be followed in planes parallel to the plane of the pattern to be computed. The separation between these planes has no particular limits. In general, making more measurements over the surface results in more accurate computed values.

Line Measurements

1. Useful data may be obtained with a suitable line hydrophone, but only if the line is used with its axis normal to the plane of the pattern to be computed.

2. A suitable line must be no more than 0.25λ in width (or diameter), and long enough for each end to extend to where amplitudes are down 20 to 30 db. Its sensitivity along its length must be uniform to within ±1 db.

3. Successive measurements with a line should be separated by no more than 0.8λ -- preferably by no more than 0.5λ.

Pulsed Measurements

1. When pulsed transmission is used it is recommended that either the probe be stopped at each measurement point while measuring, or that the pulses be initiated by a mechanical trigger which is actuated after each desired increment of probe travel. This assures that the data correspond to the correct points in space.

2. Pulse lengths should be used which are long enough for steady-state conditions to be reached during the pulse.

3. Measurements should be made during the steady-state portion of the pulse.

4. Care should be taken to measure amplitude and phase at or very near the same time during the pulse; for example, at the center of the pulse.

5. When phase is measured on a time interval meter, the start input should always be set to trigger on a zero-axis crossing in order that sufficiently accurate phase be measured regardless of amplitude changes.

Tank Measurements

1. For tank measurements the hydrophone should be placed as far from the walls as possible.

2. Reliable tank measurements cannot be made unless the steady-state condition is reached before the reflected energy from the tank walls interferes with the direct pulse. If reflected energy from the tank walls is ever a problem, it is likely that one of the two untried techniques described in Chapter IV will make possible reliable nearfield measurements.

15 March 1962
DDB/lb

C H A P T E R V I

A NEARFIELD CYLINDRICAL TRANSDUCER TEST WITHOUT COMPUTATIONS

Some work has been done on investigating the possibilities of a simplified nearfield test for a cylindrical transducer. Such a test might be made on a transducer in order to see whether it were in satisfactory condition for Fleet operation. Hopefully, such test could be performed easily and quickly without the need for computations.

It is understood that dead staves or staves wired in reverse present one of the problems normally found in unsatisfactory transducers. Nearfield measurements were made while all 48 staves of the AN/SQS-4 Mod 3 transducer were being driven. Similar measurements were made with 47 consecutive staves, 46 consecutive staves, and 45 consecutive staves. This was also done with 47 staves connected correctly and the other stave wired in reverse. Portions of the amplitude measurements for the 48-stave and 47-stave cases are shown in Dwg. AS-6530. It is seen that one dead stave is clearly detectable in the nearfield. Comparison of the two phase plots would also reveal the dead stave. In the case of a reversed stave or greater numbers of dead staves, the effect on the nearfield is even more obvious. The measurements from which the graphs were plotted were made with a line hydrophone at about 5 in. from the transducer. When these measurements were repeated with a probe hydrophone, the effect on the nearfield due to one dead stave was more pronounced than in the line hydrophone data. Thus it is felt that a dead stave can easily be detected by inspection of nearfield amplitude and/or phase measurements.

A question that comes to mind is whether one dead stave is enough to warrant condemning a transducer. This has also been studied. Since measured farfield patterns show that one dead stave causes only a small perturbation in the "omnidirectional" pattern, a 47-stave transducer would still be useful for omnidirectional operation. However, it would probably not be good for operation with a smaller group of staves. "Twelve-stave" farfield patterns

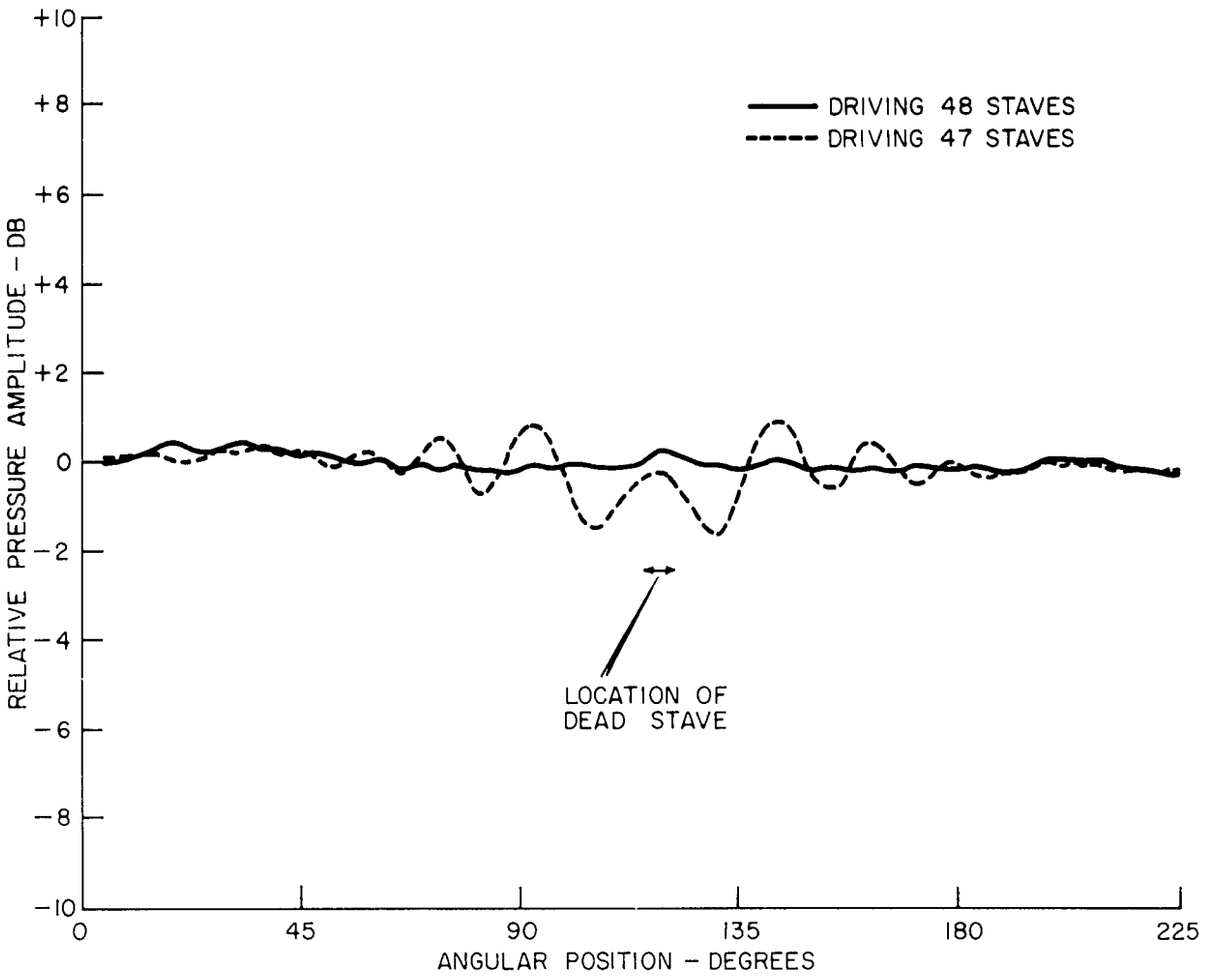

NEARFIELD PRESSURE AMPLITUDE VS ANGULAR POSITION

DRL — UT
DWG AS 6530
DDB - LRS
2 — 8 — 62

were made by wiring only eleven staves and successively leaving a dead stave in each of the twelve positions. All of these patterns were drastically different from the true twelve-stave pattern. It is reasonable to assume that similar measurements with 15 of 16 staves in operation would give similar results. It would seem from this evidence that one dead stave would be enough to warrant condemning a transducer for a beam-forming application. In fact, this evidence raises the question as to whether a transducer should be condemned if it has a smaller fault than a dead stave, such as a dead element of a stave. No farfield patterns have been made with dead portions of staves. It is reasonable that dead elements could be detected by measuring nearfield pressures around the transducer with a probe placed at several vertical levels.

It is felt that after more extensive, careful measurements it would be possible to make decisions concerning the criteria for an empirical GO/NO-GO test for such a transducer. That is, 48-stave measurements would be made with a line hydrophone or several probes. If the amplitude plots were uniform to within some limits which had been agreed upon, the directivity of the transducer would be satisfactory. If the level of the nearfield measurements was within certain limits, the source level of the transducer would be satisfactory.

It is possible that an effective test procedure that is as simple as has been described will not be found. It may be possible to examine amplitudes only, but phases may also have to be considered. The experiments made thus far indicate that the chances of developing a simple, effective test are good.

C H A P T E R V I I

SUMMARY AND CONCLUSIONS

The theory of the computation of directivity patterns and source levels of a transducer from nearfield pressure amplitude and phase data has been developed. Preliminary work with four types of transducers in open water showed good agreement between measured and computed patterns. Extensive work with an AN/SQS-4 Mod 3 transducer has been done and agreement between measured and computed patterns has been as good as ±1 db in the more recent work. This includes measurements made in open water and in a highly reflective tank. Tank measurements were made near the leading edge of the received pulse; that is, before reflections from the tank walls could interfere. The tank diameter was only 2.9 times that of the transducer. In several cases source level was computed with the patterns and proved to be within ±1 db of measured values in each case.

Some work has been done on the development of a simplified nearfield test for large low-frequency transducers. Such a test would enable one to make certain judgments about the farfield performance of a transducer from the nearfield measurements without the need for computations. The possibility of developing such a test looks promising.

15 March 1962
DDB/lb

A P P E N D I X

NUMERICAL FORMULAS AND FLOW CHARTS

Introduction

Equation (8) of Chapter I,

$$p(P) = - \frac{ik}{4\pi} \int\int_S (1 + \cos \beta) \frac{e^{ikr}}{r} p \, dS \quad , \tag{A-1}$$

was applied to the cases of the five transducers with which computations were made. Numerical formulas were developed for the specific surfaces of integration in the appropriate coordinate systems. The development of these formulas is presented. Because these formulas were evaluated on a digital computer, flow charts are also presented.

A flow chart is an outline showing the logical sequence of operations involved in the numerical evaluation of an expression. It enables a programmer to write out the coding statements for a program on any computer without difficulty. The flow chart need not be restricted to a machine application, however, for it can also be used as a procedure for hand calculations.

For the case of the dipole and AN/SQS-4 Mod 3 transducers, where the surface of integration was a right circular cylinder, an actual computer program is included.

Dipole and AN/SQS-4 Mod 3 Transducers

The first application that will be considered is for a surface of integration in the shape of a right circular cylinder. This surface of integration was used with the dipole and the AN/SQS-4 Mod 3 transducers.

A sketch of the coordinate system, the surface of integration, and the field point P is shown in Dwg. AS-6489. It is seen from the sketch that the

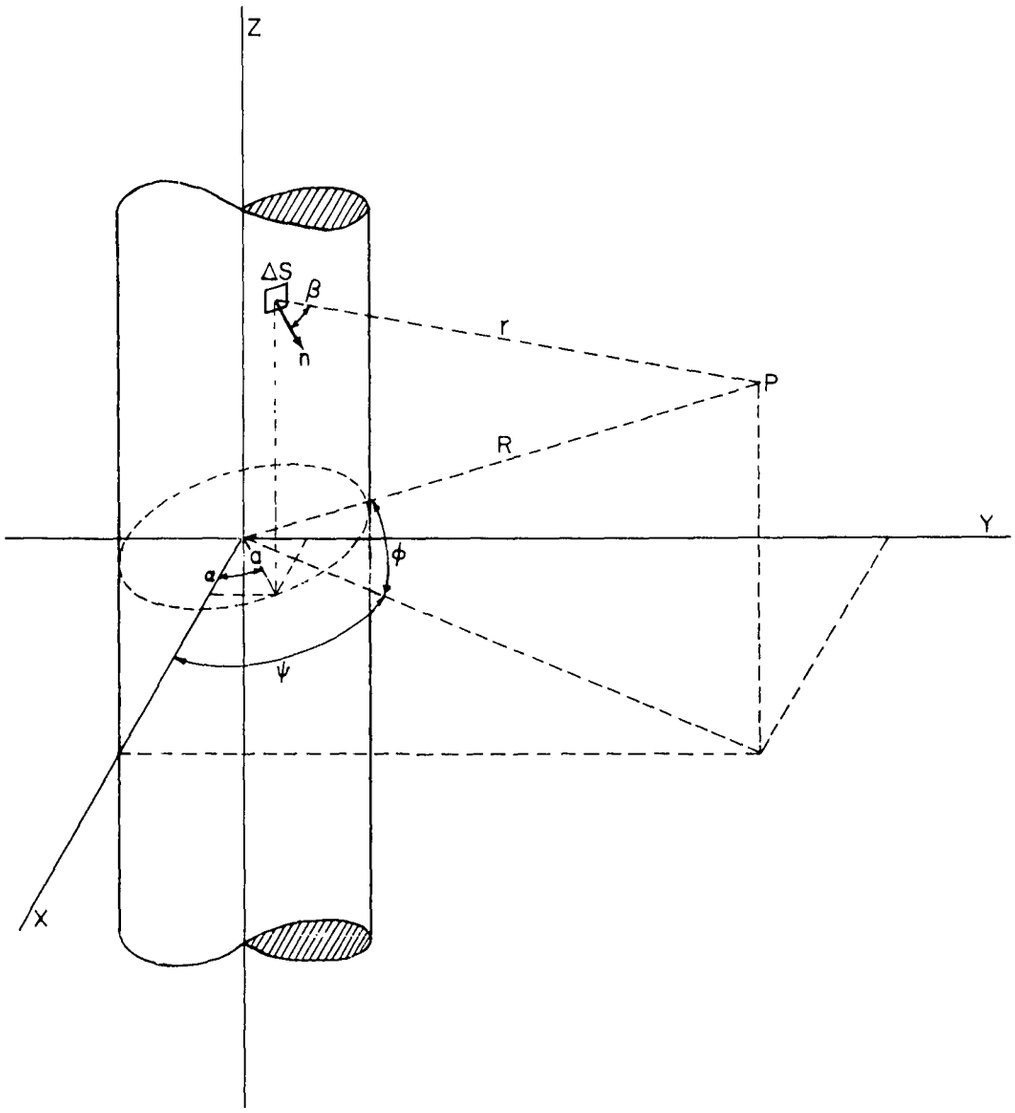

DIPOLE AND AN/SQS-4 TRANSDUCER COORDINATE SYSTEM

rectangular Cartesian coordinates of P are

$$(R \cos \varphi \cos \psi,\ R \cos \varphi \sin \psi,\ R \sin \varphi) \quad ,$$

and the coordinates of ΔS are

$$(a \cos \alpha,\ a \sin \alpha,\ z) \quad .$$

Therefore,

$$r^2 = (R \cos \varphi \cos \psi - a \cos \alpha)^2 + (R \cos \varphi \sin \psi - a \sin \alpha)^2 + (R \sin \varphi - z)^2 \quad . \qquad (A\text{-}2)$$

This reduces to

$$r^2 = R^2 + a^2 - 2aR \cos \varphi \cos(\psi - \alpha) - 2zR \sin \varphi + z^2 \quad , \qquad (A\text{-}3)$$

or

$$r = R \left[1 - \frac{2a \cos \varphi \cos(\psi - \alpha) + 2z \sin \varphi}{R} + \frac{a^2 + z^2}{R^2} \right]^{1/2} \quad . \qquad (A\text{-}4)$$

Since P is in the farfield, R is much greater than either a or z, which quantities are approximately the dimensions of the transducer. If the binomial theorem is applied and higher order terms in 1/R are neglected, the expression becomes

$$r \cong R \left[1 - \frac{a \cos \varphi \cos(\psi - \alpha) + z \sin \varphi}{R} \right] = R(1 - \gamma) \quad . \qquad (A\text{-}5)$$

Therefore,

$$r \cong R - a \cos \varphi \cos(\psi - \alpha) - z \sin \varphi \quad , \qquad (A\text{-}6)$$

and Equation (1) becomes

$$p(P) = -\frac{ik}{4\pi} e^{ikR} \iint_S (1 + \cos\beta) \frac{e^{-ik[a \cos\varphi \cos(\psi - \alpha) + z \sin\varphi]}}{R(1 - \gamma)} p \, dS \quad . \qquad (A\text{-}7)$$

Because P is in the farfield, the line of length R is approximately parallel to the line of length R. Thus cos β is very nearly equal to the cosine of the angle between the outward normal and the line of length R. This cosine is equal to the scalar product of a unit vector with components

$$(\cos\varphi \cos\psi, \cos\varphi \sin\psi, \sin\varphi)$$

and the unit normal,

$$(\cos\alpha, \sin\alpha, 0) \quad .$$

This scalar product is equal to

$$\cos\varphi(\cos\psi \cos\alpha + \sin\psi \sin\alpha) \quad ,$$

and therefore

$$\cos\beta \cong \cos\varphi(\cos\psi \cos\alpha + \sin\psi \sin\alpha) = \cos\varphi \cos(\psi - \alpha) \quad . \qquad (A\text{-}8)$$

Because of the farfield condition, the $R(1 - \gamma)$ in the denominator is approximated by R as a standard practice. These substitutions give

$$p(P) = -\frac{ik}{4\pi} \frac{e^{ikR}}{R} \iint_S [1 + \cos\varphi \cos(\psi - \alpha)] e^{-ik[a \cos\varphi \cos(\psi - \alpha) + z \sin\varphi]} p \, dS \quad , \qquad (A\text{-}9)$$

which becomes upon the evaluation of the limits of integration

$$p(P) = -\frac{ik}{4\pi}\frac{e^{ikR}}{R}\int_0^{2\pi}[1+\cos\varphi\cos(\psi-\alpha)]\,e^{-ika\cos\varphi\cos(\psi-\alpha)}$$

$$\cdot\int_{-\ell/2}^{+\ell/2} p(z,\alpha)e^{-ikz\sin\varphi}\,a\,dz\,d\alpha \quad . \qquad \text{(A-10)}$$

For the maximum accuracy attainable, the Gaussian quadrature formula[1] is used in the vertical integration with the result that

$$\int_{-\ell/2}^{+\ell/2} p(z,\alpha)e^{-ikz\sin\varphi}\,dz = \frac{\ell}{2}\sum_{n=1}^{N} A_n p(z_n,\alpha)e^{-ikz_n\sin\varphi} \quad . \qquad \text{(A-11)}$$

The other integral is evaluated by the rectangular method, and for P described by (φ,ψ,R)

$$p(P) = \left[-\frac{ik}{4\pi}\frac{e^{ikR}}{R}\frac{\ell a\Delta\alpha}{2}\sum_{m=1}^{M}\left[1+\cos\varphi\cos\left(\psi-\alpha_m\right)\right]e^{-ika\cos\varphi\cos\left(\psi-\alpha_m\right)}\right]$$

$$\left[\sum_{n=1}^{N} A_n\, p(z_n,\alpha_m)e^{-ikz_n\sin\varphi}\right] \qquad \text{(A-12)}$$

where

$$M = \left[\frac{2\pi}{\Delta\alpha}\right]$$

As explained in Chapter II, if only computations in the x-y plane ($\varphi=0$) are desired, measurements may be made with a line hydrophone of length ℓ

[1] H. Margenau and G. M. Murphy, The Mathematics of Physics and Chemistry (D. Van Nostrand Co., Princeton, 1956), 2nd Ed., p. 480.

aligned parallel to the z-axis. The data obtained with the line p $\left(\alpha_m\right)$ represent evaluations of the second summation in Equation (A-12). Thus the expression for p(P) becomes

$$p(P) = C \sum_{m=1}^{M} \left[1 + \cos\left(\psi-\alpha_m\right)\right] e^{-ika\cos\left(\psi-\alpha_m\right)} p\left(\alpha_m\right) \quad . \qquad \text{(A-13)}$$

where C is two times the constant preceding the summations in Equation (A-12).

Flow charts for the evaluation of p(P) in Equations (A-12) and (A-13) are shown in Dwgs. AS-6487 and AS-6488. The following changes in notation are used in the charts in order to simplify computer coding:

P_{nm} denotes the amplitude of $p\left(z_n,\alpha_m\right)$,

θ_{nm} denotes the phase of $p\left(z_n,\alpha_m\right)$,

P_m denotes the amplitude of $p\left(\alpha_m\right)$,

θ_m denotes the phase of $p\left(\alpha_m\right)$,

AK denotes k, and

RAD denotes a.

A subscript of o means the original angle of a sequence; f means the final angle.

Fortran coding statements for the computer evaluation of Equation (A-13) are given in the following list. Although this program was written specifically for the Control Data Corporation 1604 computer, it should be usable -- or very nearly so -- on several other machines.

Line Transducer

The previously developed expressions for the cylindrical surface can easily be modified to fit the case of a line transducer by assuming symmetry about the z-axis. A sketch of the coordinate system is shown in Dwg. AS-6538. The integral expression for p(P) in Equation (A-10) becomes

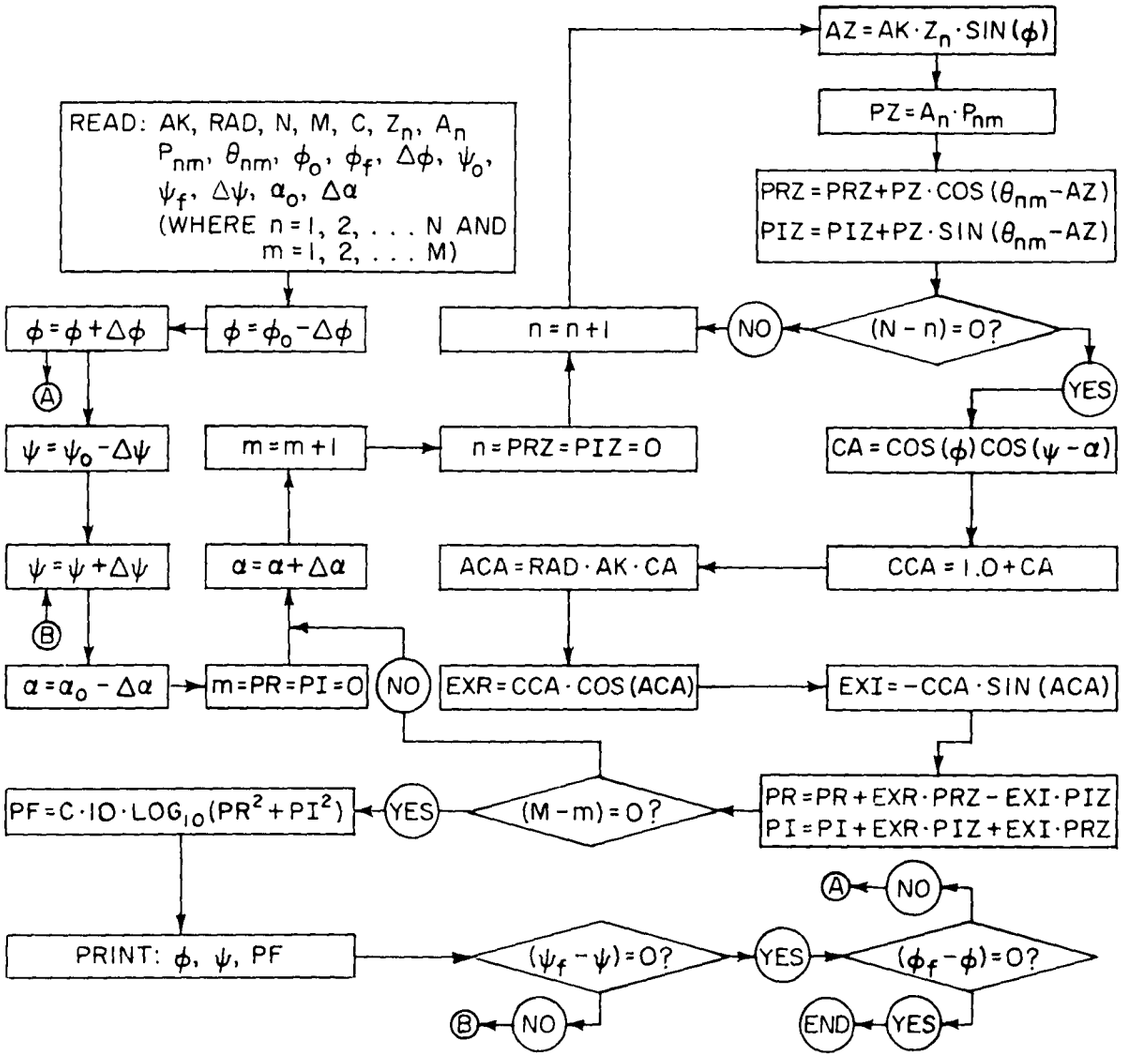

FLOW CHART FOR EQUATION (A-12)

DRL — UT
DWG AS 6487
DDB - EJW
1 - 23 - 62

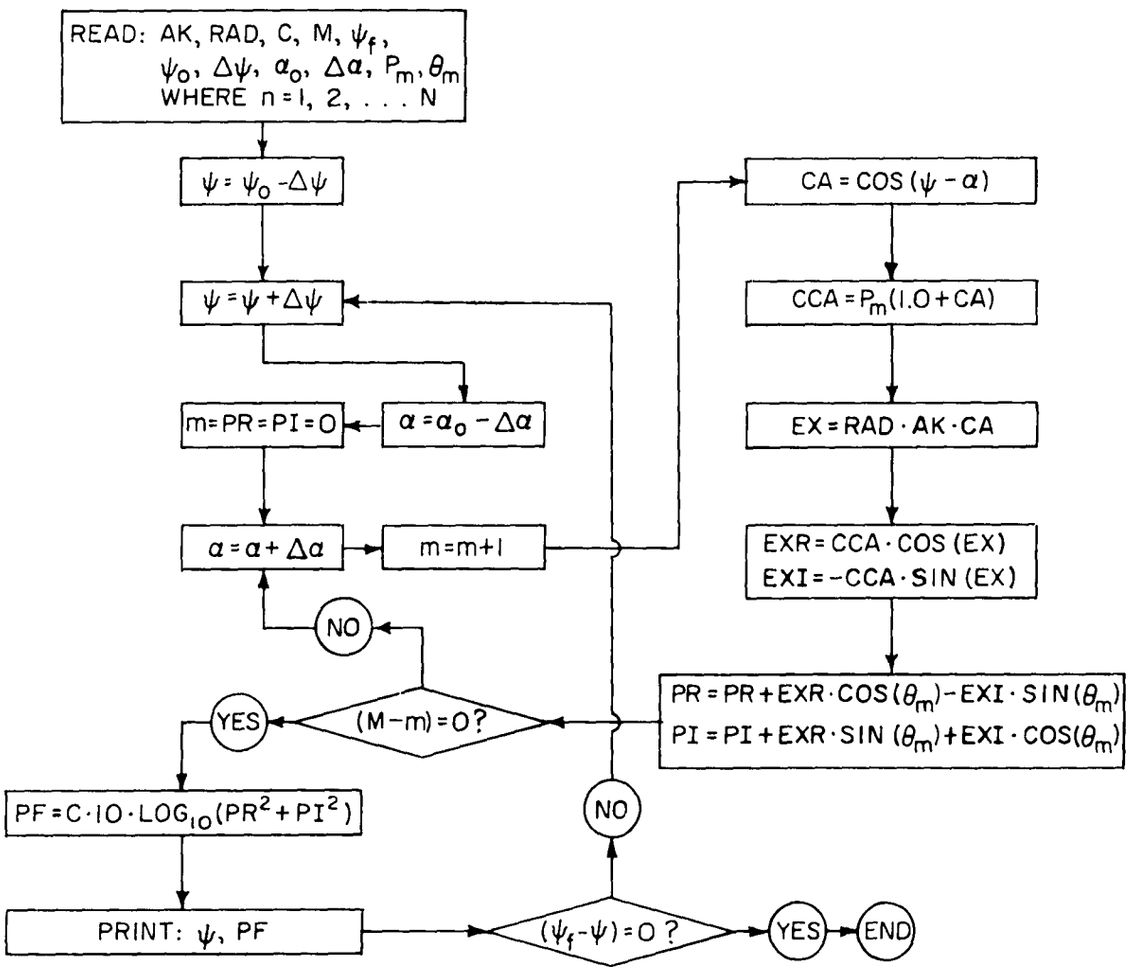

FLOW CHART FOR EQUATION (A-13)

15 March 1962
DDB/lb

FORTRAN STATEMENTS FOR THE EVALUATION OF EQUATION (A-13)

```
      PROGRAM HORIZONTAL PROGRAM
      DIMENSION P(200), THETA(200)
1     FORMAT (F5.3,1X,F4.1,1X,F8.3,1X,I3,1X,I3,1X,F6.4,1X,F6.4,1X,F6.4,1X,F6.4)
2     FORMAT (16F5.2)
3     FORMAT (10X,24H HORIZONTAL BEAM PATTERN //)
4     FORMAT (13X,4H PSI,11X,9H PRESSURE)
5     FORMAT (12X,6H (DEG),12X,5H (DB) /)
6     FORMAT (13X,F5.1,12X,F7.3)
      PRINT 3
      PRINT 4
      PRINT 5
      READ 1,AK,RAD,C,M,N,PSI0,DPSI,ALPHAO,DALPHA
      READ 2, (P(I),I=1,N)
      READ 2, (THETA(I),I=1,N)
      PSI = PSI0 - DPSI
      DO 10 I=1,M
      PSI = PSI + DPSI
      ALPHA = ALPHAO - DALPHA
      PR = 0.0
      PI = 0.0
      DO 11 J=1,N
      ALPHA = ALPHA + DALPHA
      CA = COSF(PSI - ALPHA)
      CCA = P(J)*(1.0 + CA)
      EX = RAD*AK*CA
      EXR = CCA*COSF(EX)
      EXI = CCA*SINF(EX)
      CT = COSF(THETA(J))
      ST = SINF(THETA(J))
      PR = PR + EXR*CT + EXI*ST
11    PI = PI + EXR*ST - EXI*CT
      PF = C + 10.0*LOG10F(PR**2 + PI**2)
10    PRINT 6, PSI,PF
      END
      END
```

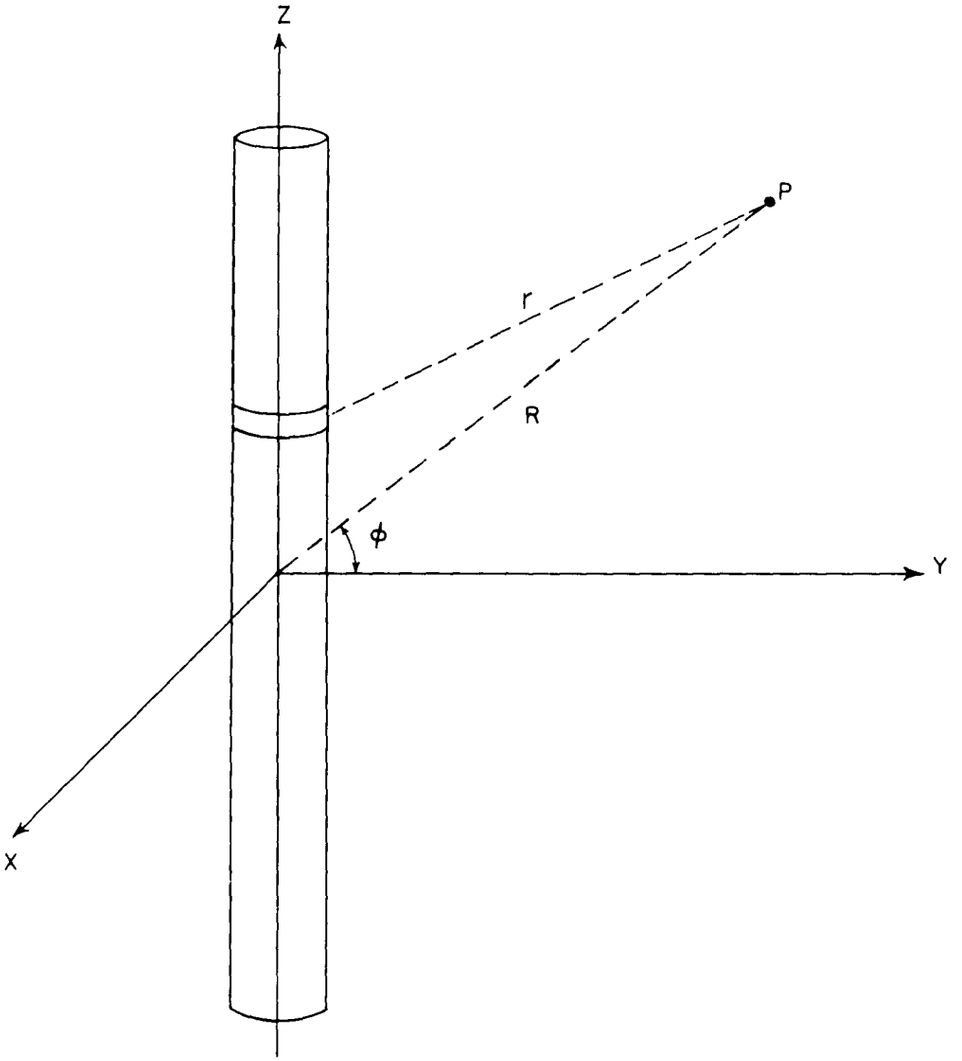

LINE TRANSDUCER COORDINATE SYSTEM

DRL - UT
DWG AS 6538
DDB - BBB
3 - 2 - 62

$$p(P) = -\frac{ik}{4\pi}\frac{e^{ikR}}{R}\int_{-\ell/2}^{\ell/2} a\, p(z)e^{-ikz\sin\varphi}\int_{0}^{2\pi}(1+\cos\varphi\cos\alpha)e^{-ika\cos\varphi\cos\alpha}d\alpha\, dz, \quad \ldots.(A\text{-}14)$$

in which p is no longer dependent upon α, and ψ has been taken to be zero due to the omnidirectionality. The integral with respect to α, which can be evaluated analytically[2], can be expressed as

$$2\pi\left[J_0(ka\cos\varphi) - i\cos\varphi\, J_1(ka\cos\varphi)\right] ,$$

where J_0 and J_1 are Bessel functions of the first and second order. The final numerical expression is

$$p(P) = -\frac{ik}{2}\frac{e^{ikR}}{R}\left[J_0(ka\cos\varphi) - i\cos\varphi\, J_1(ka\cos\varphi)\right]$$

$$\cdot\frac{\ell a}{2}\sum_{n=1}^{N} A_n\, p(z_n)e^{-ikz_n\sin\varphi} \qquad (A\text{-}15)$$

where the Gaussian quadrature formula is used again for the integration along the line.

The following changes are made in the notation for agreement with the flow chart shown in Dwg. AS-6584:

AK denotes k,

P_n denotes amplitude of $p(z_n)$,

θ_n denotes phase of $p(z_n)$, and

BESSEL [X,Y] denotes a subroutine for calculation of the Bessel function of order X with argument Y.

---

[2] N. W. McLachlan, Bessel Functions for Engineers (University Press, Oxford, 1934), pp. 43 and 51.

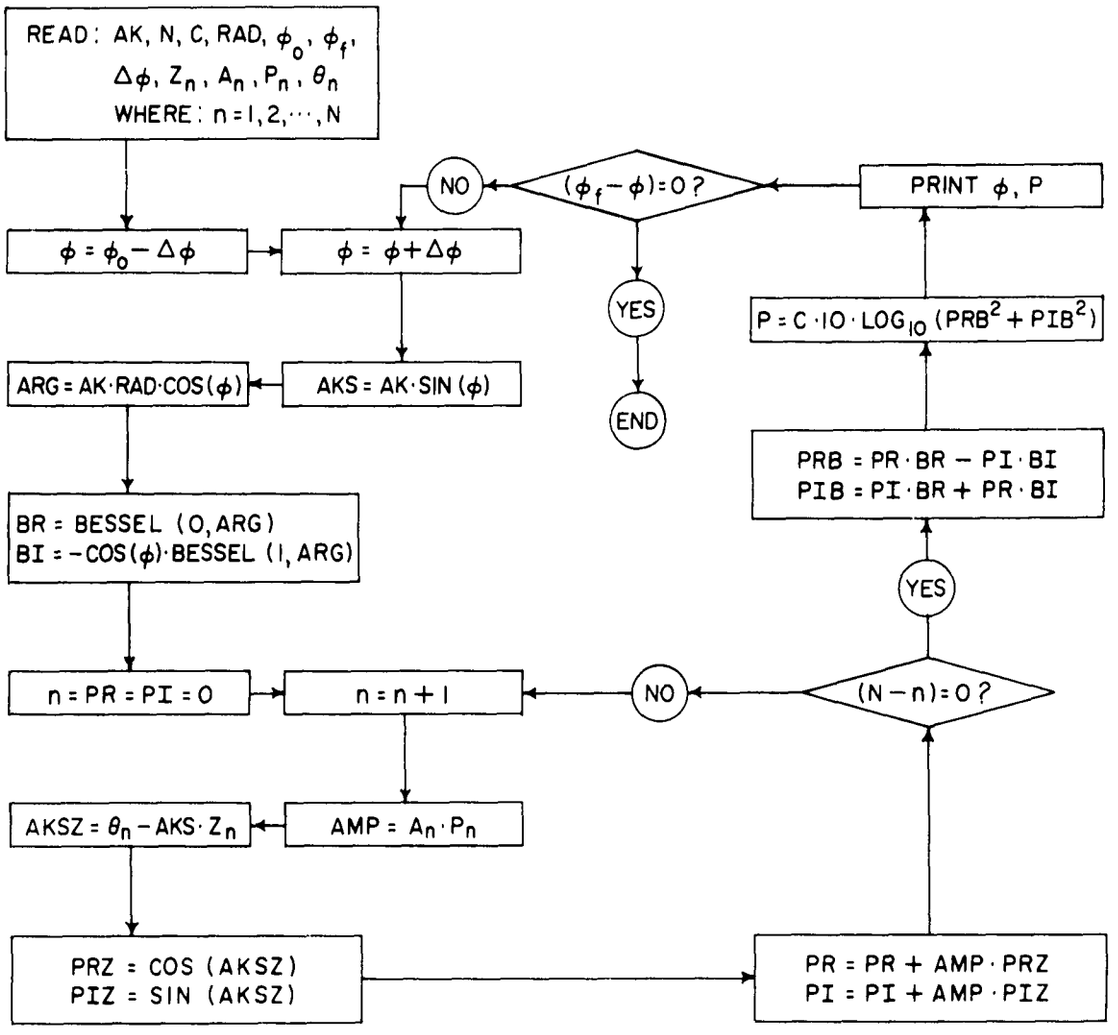

FLOW CHART FOR EQUATION (A-15)

DRL − UT
DWG AS 6584
DDB − PPR
3 — 5 — 62

Plane Array Transducer

The case of a pillow transducer or any other system which can be adequately described by a plane array of points will now be considered. The geometry is shown in Dwg. AS-6582. The coordinate system is a rectangular Cartesian one, in which the element of surface is located at the point

$$(x,\ 0,\ z) \quad ,$$

and the coordinates of P are

$$(R \cos \alpha \cos \varphi,\ R \cos \alpha \sin \varphi,\ R \sin \alpha) \quad .$$

It follows that

$$r = \left[(R \cos \alpha \cos \varphi - x)^2 + (R \cos \alpha \sin \varphi)^2 + (R \sin \alpha - z)^2 \right]^{1/2} \tag{A-16}$$

which after expansion and collection of terms becomes

$$r = R \left[1 - 2 \frac{x \cos \alpha \cos \varphi + z \sin \alpha}{R} + \frac{x^2+z^2}{R^2} \right]^{1/2} \quad . \tag{A-17}$$

Now the large R approximation and the binomial theorem may be applied as was done in the section about the right circular cylinder. The result is

$$r \cong R - x \cos \alpha \cos \varphi - z \sin \alpha \quad . \tag{A-18}$$

The direction cosine at the surface element is defined by

$$\cos \beta = \frac{\vec{r} \cdot \vec{n}}{|r|} = \frac{R \cos \alpha \sin \varphi}{|r|} \cong \cos \alpha \sin \varphi \quad . \tag{A-19}$$

Substitution into the integral equation gives

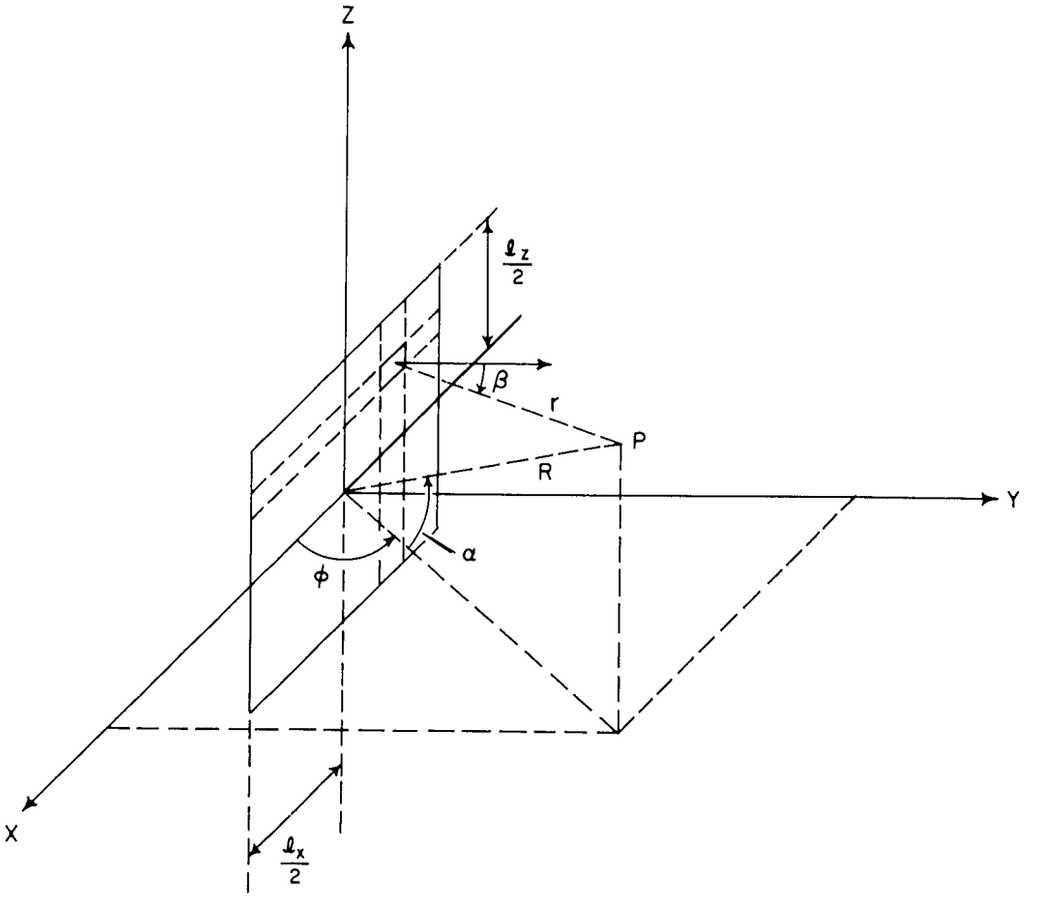

PLANE ARRAY TRANSDUCER COORDINATE SYSTEM

DRL – UT
DWG AS 6582
DDB – PPR
3 – 2 – 62

$$p(P) = -\frac{ik}{4\pi}\frac{e^{ikR}}{R}\iint_S (1+\cos\alpha\sin\varphi)e^{-ik(x\cos\alpha\cos\varphi + z\sin\alpha)}\,p\,dS \qquad (A\text{-}20)$$

where the r in the denominator has been further approximated by R. The element of area is expressed by

$$dS = dx\,dz \qquad (A\text{-}21)$$

of which each of the angles α and φ is independent. Hence

$$p(P) = -\frac{ik}{4\pi}\frac{e^{ikR}}{R}(1+\cos\alpha\sin\varphi)\int_x e^{-ikx\cos\alpha\cos\varphi}\int_z p(x,z)e^{-ikz\sin\alpha}dz\,dx \quad . \qquad \ldots. \quad (A\text{-}22)$$

The Gaussian quadrature formula is applied to each of the line integrals so that

$$p(P) = -\frac{ik}{4\pi}\frac{e^{ikR}}{R}\frac{\ell_x\ell_z}{4}(1+\cos\alpha\sin\varphi)\sum_{n=1}^{N} A_n e^{-ikx_n\cos\alpha\cos\varphi} \cdot \sum_{m=1}^{M} B_m\, p\left(x_n,z_m\right) e^{-ikz_m\sin\alpha} \qquad (A\text{-}23)$$

For agreement with the flow chart shown in Dwg. AS-6585, the following changes must be made in the notation:

AK denotes k,

P_{nm} denotes the amplitude of $p\left(x_n,z_m\right)$, and

θ_{nm} denotes the phase of $p\left(x_n,z_m\right)$.

Line-and-Cone Transducer

The line-and-cone transducer is a simplification of the plane array considered previously. This formulation will also apply to any plane array

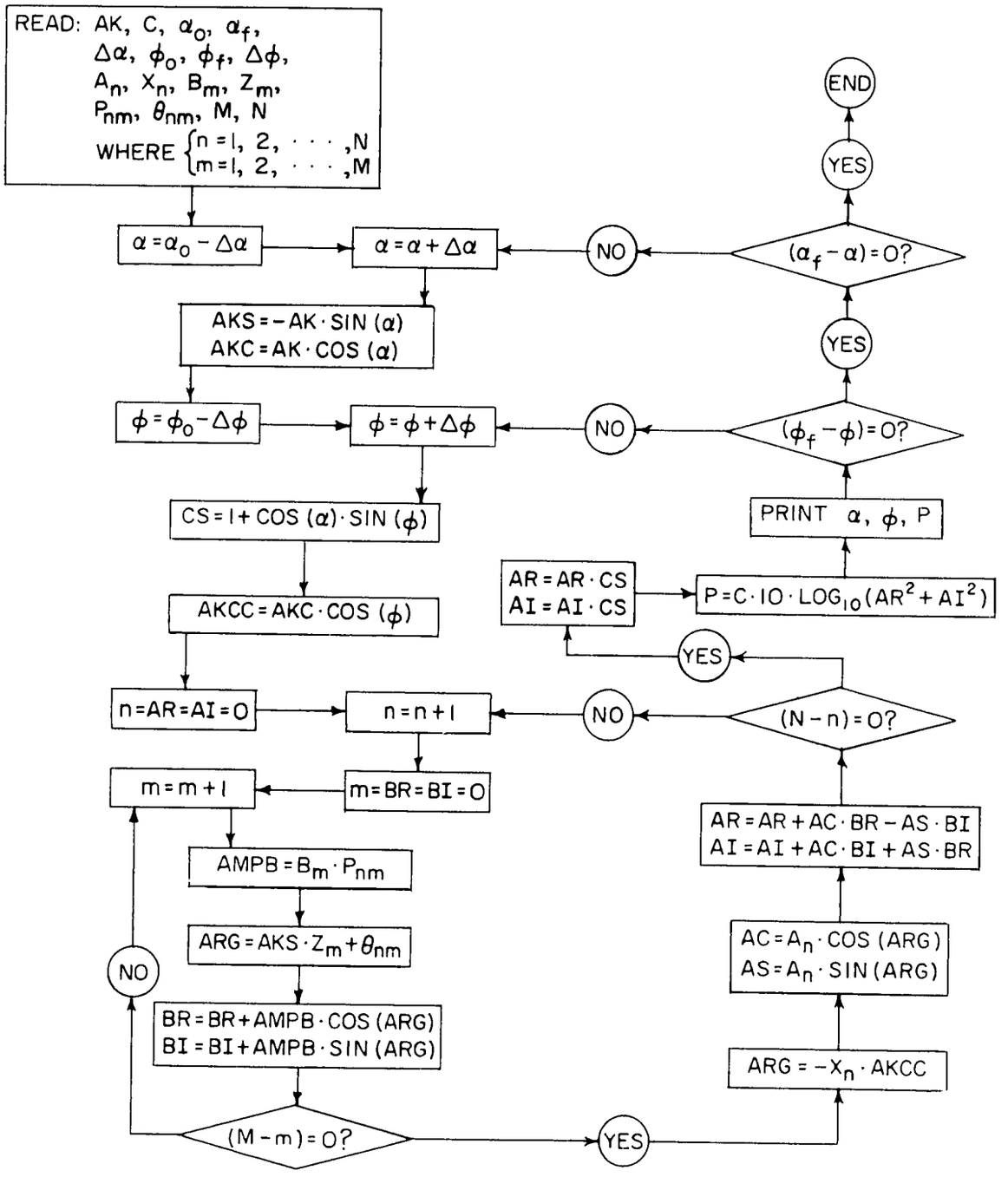

FLOW CHART FOR EQUATION (A-23)

which has symmetry about an axis normal to the plane. The parameter α will be set equal to zero, since farfield patterns in all planes containing the y-axis are identical. With the substitution, $x = \rho \cos \gamma$ (see Dwg. AS-6583), Equation (A-22) becomes

$$p(P) = - \frac{ik}{4\pi} \frac{e^{ikR}}{R} \iint_S (1+\sin \varphi) e^{-ik \rho \cos \gamma \cos \varphi} p(\rho) \rho \, d\rho \, d\gamma \quad . \tag{A-24}$$

The rectangular method of integration is used for the γ variable and the Gaussian quadrature for the ρ variable. Hence

$$p(P) = - \frac{ik}{4\pi} \frac{e^{ikR}}{R} (1+\sin \varphi) \frac{\ell}{2} \Delta \gamma \sum_{n=1}^{N} A_n \rho_n p\left(\rho_n\right) \cdot \sum_{m=1}^{M} e^{-ik \rho_n \cos \gamma_m \cos \varphi} \quad . \tag{A-25}$$

To agree with the flow chart shown in Dwg. AS-6586, changes must be made in the notation as follows:

AK denotes k,

P_n denotes the amplitude of $p\left(\rho_n\right)$, and

θ_n denotes the phase of $p\left(\rho_n\right)$.

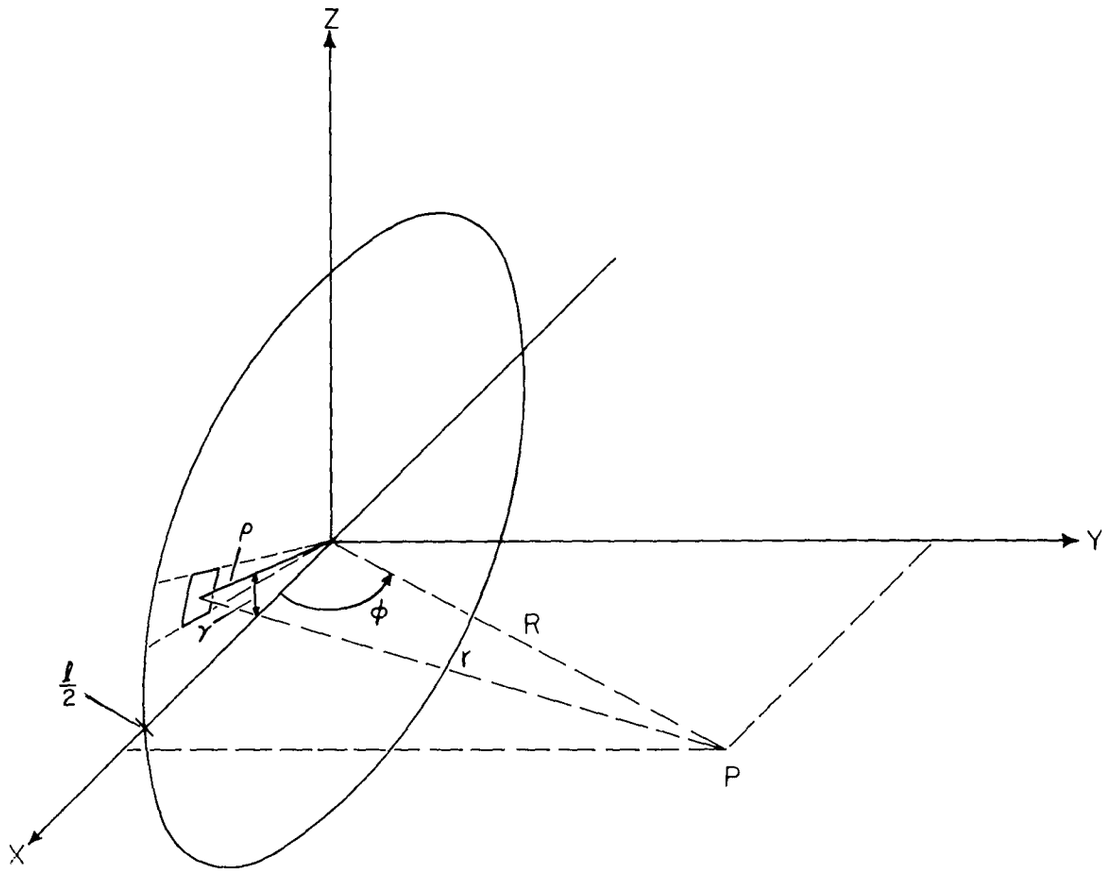

LINE AND CONE TRANSDUCER COORDINATE SYSTEM

DRL - [illegible]T
DWG A36583
DDB - LFH
3 - 2 - 62

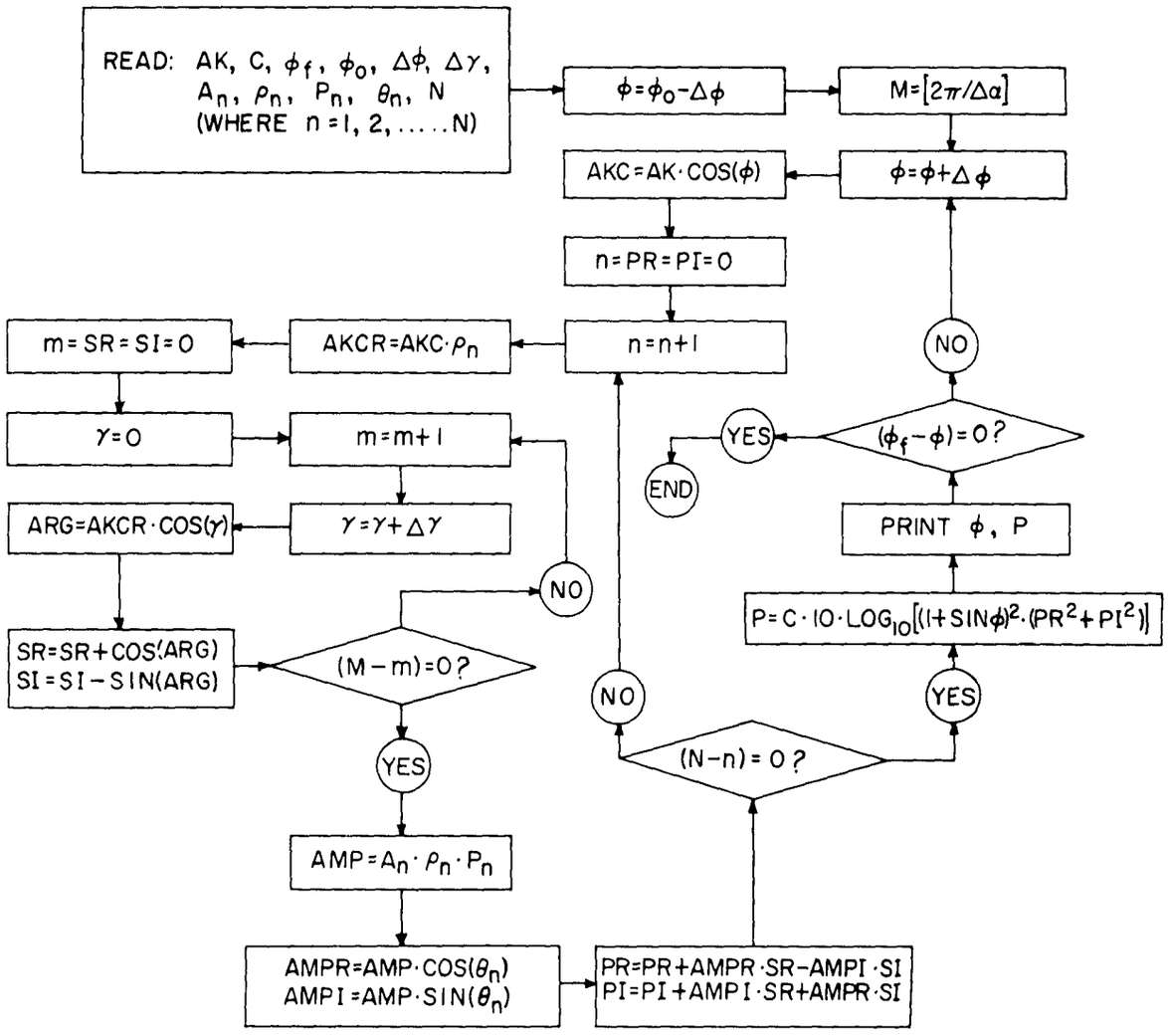

FLOW CHART FOR EQUATION (A-25)

DRL - UT
DWG AS6586
DDB - LFH
3 - 6 - 62

B I B L I O G R A P H Y

Baird, D. L., An Experimental Investigation of an Underwater Sound Transducer-Reflector Combination, Master's Thesis, The University of Texas, January 1962.

Baker, B. B. and E. T. Copson, The Mathematical Theory of Huygens' Principle (Clarendon Press, Oxford, 1950), 2nd Ed., p. 26.

Ballantine, S., "An Operational Proof of the Wave-Potential Theorem, with Applications to Electromagnetic and Acoustic Systems," J. Franklin Inst., 221, April 1936, pp. 469-484.

Design and Construction of Crystal Transducers, Summary Technical Report of Division 6 NDRC, Vol. XXII, p. 137.

Horton, C. W. and G. S. Innis, "The Computation of Farfield Radiation Patterns from Measurements Made Near the Source," J. Acoust. Soc. Am., 33, July 1961, pp. 877-880.

Innis, G. S. and C. W. Horton, Defense Research Laboratory Acoustical Report No. 172 (CONFIDENTIAL), Contract NObsr-72627, June 1960.

McLachlan, N. W., Bessel Functions for Engineers (University Press, Oxford, 1934), pp. 43 and 51.

Margenau, H. and G. M. Murphy, The Mathematics of Physics and Chemistry, (D. Van Nostrand Company, Princeton, 1956), 2nd Ed., p. 480.

Trott, W. J., Transducer Calibration from Nearfield Data, Underwater Sound Reference Laboratory Research Report No. 55, Orlando, Florida, October 1961.

DISTRIBUTION LIST

Copy

1. Chief, Bureau of Ships, Code 689A
2. Chief, Bureau of Ships, Code 689B
3-4-5. Chief, Bureau of Ships, Code 689B
6. Chief, Bureau of Ships, Code 631
7. Chief of Naval Operations, OpNav 922G
8-9. Chief, Bureau of Naval Weapons, Code RUDC-6
10. Office of Naval Research, Code 411
11-12. Office of Naval Research, Code 463
13. Commander, Submarine Development Group TWO
14. Commander, Submarine Force Pacific Fleet
15. Commanding Officer and Director, U. S. Navy Electronics Laboratory
16-17. Commanding Officer and Director, U. S. Navy Underwater Sound Lab.
18-19. Commanding Officer, Naval Air Development Center, Johnsville, Pa.
Attn: NADC Library
20. Director, U. S. Naval Research Laboratory
21. Director, U. S. Naval Research Laboratory, Code 5530
22. Director, U. S. Naval Research Laboratory, Code 1045
23. Director, U. S. Naval Research Laboratory, Code 2021
24. Commander, U. S. Naval Ordnance Laboratory
25-26. British Joint Services Mission (Navy Staff)
27. Canadian Joint Staff
28. Director, Marine Physical Laboratory
29. Research Analysis Group, Brown University
30. Columbia University, Lamont Geological Observatory
31. Director, Woods Hole Oceanographic Institution
32. Applied Physics Laboratory, The Johns Hopkins University
33. Commanding Officer, U. S. Navy Mine Defense Laboratory
34. C. O. and Dir., U. S. Navy Electronics Laboratory
Attn: Arthur Roshon
35. C. O. and Dir., U. S. Navy Electronics Laboratory
Attn: Dr. G. H. Curl, Code 2230
36. Sangamo Electric Company, Attn: C. H. Lanphier
37. Division of Oceanography, Hydrographic Office, Washington 25, D. C.
38. General Electric Company, Syracuse, N. Y.
39. Committee on Undersea Warfare, National Research Council
40. Ordnance Research Laboratory, The Pennsylvania State University
41. C. O., U. S. Navy Mine Defense Laboratory, Attn: Dr. J. Hagemann
42. C. O., U. S. Navy Mine Defense Laboratory, Attn: R. J. Urick
43. U. S. Naval Ordnance Test Station, Pasadena, California
Attn: Pasadena Annex Library
44. Commander, Mine Force, U. S. Atlantic Fleet, U. S. Naval Minecraft Base, Charleston, South Carolina
45. C. O., Key West Test and Evaluation Detachment, Key West, Florida

DISTRIBUTION LIST (CONT'D)

Copy

46. U. S. Navy Postgraduate School, Monterey, California
47. VITRO Corporation of America, Silver Spring Laboratory
48. Edo Corporation, Attn: Dr. W. R. Ryan
49. Applied Physics Laboratory, University of Washington, Seattle, Wash.
50. Commander, Mine Force, U. S. Pacific Fleet, U. S. Naval Station, Long Beach, California
51. Commander, Harbor Defense Unit, Norfolk, Virginia
52. Department of the Navy, Office of the Chief of Naval Operations (Op-315E), Washington 25, D. C.
53. Director, Engineer Research and Development Laboratories, Fort Belvoir, Virginia, Attn: Mine Detection Branch, Mr. Chandler Stewart
54. Operations Evaluation Group, Navy Department, Op03EG, Washington 25, D. C., Attn: Dr. L. E. Channel
55. Stanford Research Institute, Menlo Park, California Attn: Dr. Vincent Salmon
56. Director, U. S. N. Underwater Sound Reference Laboratory, P. O. Box 8337, Orlando, Florida
57. Institute for Defense Analyses, Communications Research Division, von Neumann Hall, Princeton, New Jersey
58. Bureau of Naval Weapons, Code RU-222 (Oceanographer), Washington 25, D. C.
59. ONR, Special Representative, The University of Texas
60. Director, DRL
61. C. M. McKinney
62. D. D. Baker
63. L. D. Hampton
64. H. V. Hillery
65. C. W. Horton
66. L. A. Jeffress
67. E. L. Klein
68. R. H. Wallace

69-70. Library, DRL